DIFFUSION COEFFICIENT OF PARTICLES IN LATTICES WITH RANDOM-BARRIERS AND WIDE DISTRIBUTION OF TRANSITION RATES

A THESIS

PRESENTED TO

THE SCHOOL OF GRADUATE STUDIES OF THE

ADDIS ABABA UNIVERSITY

IN PARTIAL FULFILIMENT OF

THE REQUIREMENT FOR THE DEGREE

MASTER OF SCIENCE IN PHYSICS

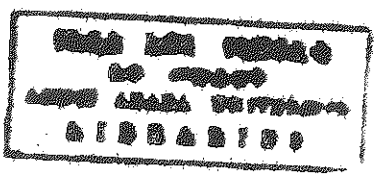

BY

HAILEMARIAMAMBAYE

JUNE 1995

Dedication

The work is totally dedicated to my father Ato Ambaye Desta and my mother W/o Mebrat Kidanu for educating their children.

Acknowledgement

Thanks are due to my advisor Prof. K. W. Kehr in Germany - KFA, who has been guiding, assisting, making close numerous disscusions, pointing out relevant literatures, and making crtical reading of the manuscript. I am thankful to Dr. S. Kotelnikov - my local advisor and Dr. I. M. Kashirsky for their unreserved cooperation and disscusion. I would like to express my sincere gratitude to Prof. P. Argyrakis for fruitful discussions and helpful comments he made in his brief stay in Germany-KFA. T. Wichmann and C. Jansen are also gratefully acknowledged for the hospitality extended to me and technical support in typing my thesis.

My thanks goes to forschungszentrum for hosting the research and offering me full benefit of the facilities required for my work. Thanks are also due to DAAD for granting financial support of my stay both in Germany and in Ethiopia.

Abstract

We have investigated the mean-square displacements of particles that perform random walks in two and three-dimensional lattices with random barriers with uniform distributions of activation energies. The lattice we considered is a mathematical lattice. For the same model Avramov, Milchev, and Argyrakis [phys.rev.E 47 2303 (1993)] discussed the crossover between anomalous and normal diffusion, but they did not Analyze the behavior of the mean-square dispalcements at long times where normal diffusion occurs. We point out that the asymptotic diffusion coefficients are well described by the effective-medium theory in the range of parameters investigated; they are in disagreement with the predictions of critical-path arguments in dimension d=3.

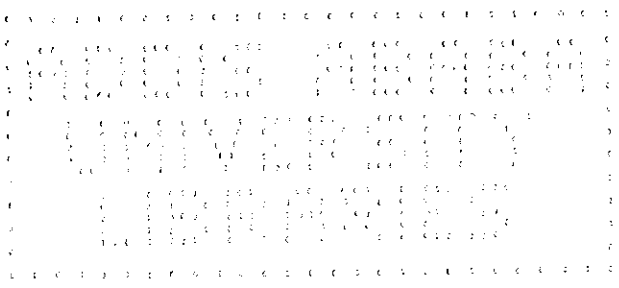

1 Contents

1 Introduction

Diffusion of a particle is described by stochastic methods. That is, probability concepts are used and the information about the particle dynamics is contained in a statistical quantity called a probability distribution on the lattice. The dynamics is formulated either in terms of enumerating the individual transitions of the particle from one site to another (random walk description) or interms of rate equations for the probability ditribution, the so called master equation.

The justification of the stochastic methods must be sought in the complicated Hamiltonian dynamics of the particle. The particle is coupled to the many degrees of freedom of the lattice and it undergoes rapid and irregular momentum changes by its interaction with the atoms in its environment. As this statement implies, there must be a wide separation of time scales between the particle motion and the lattice vibrations; the host atoms then act as a random heat bath coupled to the particle. In solids, the local minima of the potential form a lattice on which the particle moves. The particle remains near a local minimum of the potential energy for a long time and in an event of short duration it passes through a local saddle point of the potential to get in to the next local minimum. Thus there is a second separation of time scales between the duration of the transitions and the mean residence time of the particle near the local minima. It is this second separation that allows the passage to a description of particle diffusion in solids as a random walk between lattice points. Theories that deduce the transition rates between local minima from a combination of Hamiltonian mechanics and statistical mechanics have been developed /1,2/.

Stochastic modelling is quite powerful and the methods have been used with great success in Laser theory/3/, Biological systems/4/, and Chemical dynamics. Considerable progress has been achieved in the last years in the direct treatment

of random walks in disordered lattices. This progress is partially due to the identification of prototype models of particle diffusion in disordered solids; for instance the random-barrier and the random-trap model. Both models have disorder only in the transition rates and the paticle diffuses on a regular lattice.

Diffusion in disordered systems often does not follow the classical laws which describes transport in ordered crystalline media, and this leads to many anomalous physical properties.

The problem of diffusion in disordered media is part of the general problem of transport in disordered media. The range of applicability and physical interest is enormous. Most of the materials encountered in nature in every day experience are non-crystalline, disordered materials. The classic theories of transport valid for crystals do not apply, and the physics of transport, in particular diffusion, is more complicated in these disordered systems. Some typical examples are the problems of the transport properties in fractured and in porous rocks, the anomalous density of states in randomly dilute magnetic system in silica aerogels and in glassy ionic conductors , anomalous relaxation phenomena in spin glasses /5-7/ , conductivity of superionic conductors such as hollandite and of diffusion -controlled fusion of exitations in porous membrane films , polymeric glasses and isotropic mixed crystals /6-9/, to mention a number of examples. In the review /10/ a large range of real situations in which randomness is a central aspect of the problem is discussed. It is during the 80's the subject has evolved rapidly, and both theoretical and experimental interest in materials with randomness in their properties has increased substantially. On the theoretical side the reasons are; the development of computers capable of determining information about reasonably large models of random systems, new efforts towards understanding the topological structure of random materials, both by physical model construction and by computer simulation /11/.

The theory of random walk has been applied in many areas of science, especially as a model for transport phenomena. The mean-square displacement of a random walker, $\{R(t)^2\}$, is proportional to the time t , $\{R(t)^2\} \sim t$, for any number of spatial dimension d (Einstein's law). However in disordered systems, this law is not valid in general. Rather, the diffusion law becomes /6,12/:

$$\{R(t)^2\} \sim t^{\frac{2}{d_w}} \tag{1}$$

with $d_w \geq 2$. That is, there are cases with $d_w > 2$ as well as with $d_w = 2$. This slowing down of the transport is caused by the delay of the diffusing particles in dangling ends, bottlenecks and so on existing in the disordered structures.

Many models have been developed to study the diffusion coefficient in disordered systems. Most notably, disordered systems have been modelled by regular lattices with a random distribution of transition rates or bond conductivities. Moreover, randomness may be viewed as being imposed by either "dynamic" or "static" disorder. In the first case the renewal of the barriers occurs upon each jump of the tracer because the local environment is formed by particles, identical with the hopping one and performing the same kind of motion. Evidently, this case is more appropriate for describing self diffusion. In the "static" case one deals with a frozen lattice of random barriers and a tracer atom moves without changing them. This model has been treated extensively in the literature, see /13/, and is believed to describe diffusion and mobility of foreign particles. In this work we tried to determine the diffusion coefficient of a single particle that diffuses in static disordered lattices for a particular model, the Random Barrier Model (RBM), where we have randomly distributed barrier energies between the sites. The sites are at the potential minima and the barriers which the particle should surmount have heights which are randomly and independently placed on the lattice according to a uniform distribution $\nu(E)$. The energy required for the particle to overcome the barrier is named as

Activation Energy. The transition rates from site i to site $i+1$, $\Gamma_{i,i+}$, is related to the activation energy by the Arrhenius law,

$$\Gamma = \Gamma_0 \exp(-\frac{E}{K_B T}) \qquad (2)$$

for simplicity we ignore the indices in the above expression. The transitions from site i + 1 to i have the same rate as the ones from i to i+ 1. This feature is present because all the minima lie at the same energy /13/ when no bias is present. As might be expected from the pictorial representation fig.1 below, which shows the random barrier model in one dimension, the equilibrium solution corresponds to all sites having the same occupation probability. But we are not going to solve the master equation for the disordered model, rather we implement Monte Carlo simulations.

We intend to study diffusivity of a single particle at different temperatures. In a Monte Carlo simulation, the concept of a temperature makes no sense. The behavior of the diffusing particle in the specified model is determined by the dimensionless parameter $\alpha = \frac{K_B T}{E^*}$, the ratio of thermal activation energy to the height of the barrier. Simulations and analytical calculations for α eq uals 1, 0.5, 0.2, 0.1, and 0.05 to determine the diffusion coefficient have been done. When α is 1, that is when the thermal activation energy approaches the height of the barrier almost all particles contribute to the diffusivity. In the low temperature limit almost all particles can be considered as ``frozen", that is they do not have enough thermal energy to overcome the barrier.

In our work two or more particles could occupy the same lattice site without feeling the presence of one another. To achieve good statistics and to reduce the noise we considered a large ensemble of particles in our simulation typically 25,600 particles. Simulations up to 10^5 have been performed for small temperaure values (α values). Large Monte Carlo steps will get you in to the asymptotic regime of diffusion, where the mean-square displacement is

proportional to t. In the Monte Carlo simulation we monitored the mean–square–displacement in the diffusivity program and we have considered also the influence of a bias where the particle is forced to drift in a particular direction (making biased random walk). Considering the linear response and using the Einstein relation we calculate the mean displacement analytically and compare it with the Monte carlo simulation of the mobility.

Analytical calculations are also made to solve the Effective Medium Approximation (EMA) for a particular distribution of barrier energies. We employ the effective–medium approximation to obtain an average description of transport in those random systems. An exact result is available for the RBM and other lattice models of disorder in one dimension, see /13,14/. Expressions and explicit values for the diffusion coefficient are obtained for one, two and three dimensions. These results are compared with results from simulations of both mobility and diffusivity.

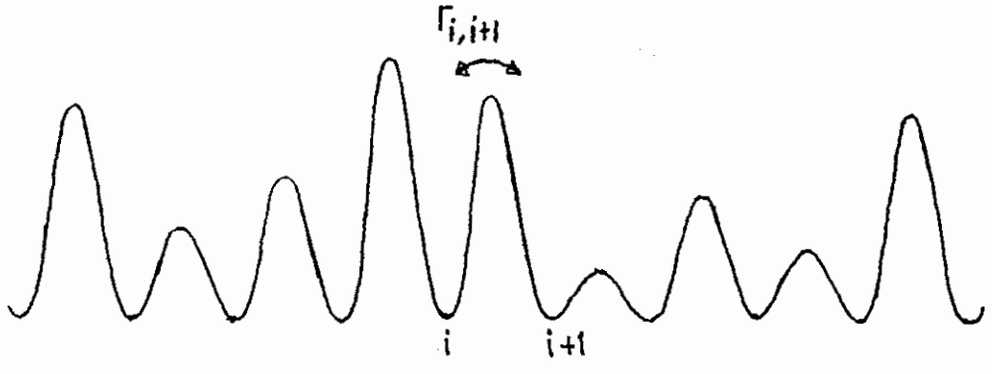

Figure 1: Pictorial representation of random barrier model in one dimension. The particle resides in one of the valleys, all valleys have the same depth. The rate at which a particle hops over a barrier is reduced as the peak is increased. Barriers of differing heights are independently distributed.

In section 2 , we describe the effective medium approximation. We derive the

self consistency condition using the Effective-Medium Theory. As it is normally done in other cases we start deriving results for one dimension, and extend them to two and d-dimensions. The mean-square displacement is also derived here. In section 3 the theoretical model is described. Using this model we solve the self consistency condition to find analytical expressions for the diffusion coefficient in one, two, and three dimensions. In section 4 we describe a different prediction of the diffusion coefficient from percolation theory. In section 5, the Monte Carlo simulation which is our main tool is discussed. Results of simulations for one, two, and three dimensions are described in section 6 and compared with predictions of EMT. Section 7 contains concluding remarks, in particular a discussion on the validity of EMT, compared to the prediction derived from percolation arguments.

2 Effective - Medium Theory for random barrier model

The Effective Medium Theory is the most utilized theory in our work. The analytical calculation of diffusion coefficients for our model are basically made by solving the self consistency condition, which is actually the main result of this theory. Our simulation results for diffusivity and mobility will then be compared with it. So, it is reasonable to discuss first the sense of this theory.

In this theory you imagine of an ideally perfect structure, like an ideal crystal. For illustration purpose, consider the random barrier model, with all the barriers effectively of the same height distribute through the system. However, the diffusive behavior in this system is characterized by a transition rate, which is not a stochastic variable. It is a definite function of time which this theory is aimed to determine. Now we have what is called the effective medium. The problem now is that systems in our surrounding are not as perfect as it is imagined above. People became interested in developing a method to reconcile the ideal system with at least part of reality, and they came up with the Effective Medium Approximation. For example, as an approximation to disordered random barriers, you embed one stochastic variable taken from a common distribution in to the effective medium and take the ensemble average over the distribution. A simpler formulation is given by the analytical implementation of the embedding procedure which was described above. Their merit lies in the ease of calculating explicit results within the formalism /13,15-17/.

The Effective - Medium Approximation is one simple method which can give reasonable results in any dimension d. The reliability of the EMA can be gauged bycomparison with exact results and checking the solution against Monte - Carlo

simulations. Results from EMT have been seen to agree with exact results. Luck has discussed the accuracy of this theory by comparing it with results of percolation expansion for conductivity of random resistor networks /17/.

The Effective Medium Theory is applicable to a wide class of systems. For example Kirkpatrick has used this theory for resistor network models to calculate the conductance and anmd arrived at the same expression for the self - consistency condition as is obtained for the Random Barrier Model (RBM) and other similar models /18/.

In this section we develop the effective medium description of the RBM. This model is defined by aset of transition rates $\{\Gamma_{nn'}\}$. $\{\Gamma_{nn'}$ is the transition rate from site n to the nearest neighbor site n'. In the random barrier these rates have the symmetry $\Gamma_{nn'} = \Gamma_{n'n}$ Our first aim is to find a self - consistency expression for the average transition rate. That is , we calculate the conditional probability when an average is taken over the distribution of the transition rates, {P(n,t)}. The initial conditions for the disordered - averaged conditional probability, or the effective medium probability are the uniform occupation $P(n,0;m,0) = \delta_{nm}$, that is the particle starts at each site with equal probability for each realization of the set $\{\Gamma_n\}$ on the lattice. The approximate effective medium transition rates $\Gamma(t)$ must be determined self - consistently from an embedding procedure /16,19,20/.

2.1 Derivation of self consistency condition for one dimensional lattice with one stochastic barrier

To begin with, we choose a cluster of bonds in the lattice that have specified rate $\Gamma_{nn'}$ taken from $\rho(\Gamma)$, distribution of transition rates . This cluster is embedded into an effective medium composed of $\Gamma(t)$ between the nearest neighbors. The simplest cluster consists of just one bond, as it is depicted in fig.2. We will use this single bond approximation through out this work. The conditional probability for this medium with a fixed

bond $\Gamma_{nn'}$ embedded in it will be designated by $P(n,t;m,0)$ and it also has the initial condition $P(n,t;m,0) = \delta_{nm}$. For simplicity we use the notation $P_n(t) = P(n,t;0,0)$ in the rest of the work. The site $m = 0$ is designated as the initial site . For the random barrier model the transition rates from site, $n = 0$ to site $n = 1$ at the other end of the bond, will be the random transition rate Γ'; on the other hand, the transition rate from any site n to $n-1$ outside the cluster is $\Gamma(t)$.

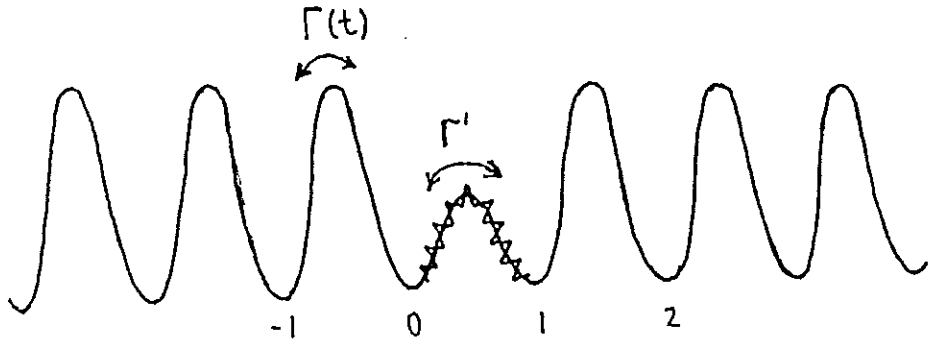

Figure 2: One dimensional lattice with one stochastic barrier embeded in an effective medium. The stochastic barrier is indicated by the crosses on top of it.

Imagine now one-dimensional lattice where every bond has the time-dependent effective-medium transition rate $\Gamma(t)$. The conditional probability of finding a particle at site n at time t in this effective-medium lattice will be designated $E_n(t)$. The initial condition is also$E_n(0) = \delta_{nm}$. The quantity $E_n(t)$ satisfies the master equation

$$\frac{\partial E_n}{\partial t} = \int dt' \, \Gamma(t-t')[E_{n+1}(t') + E_{n-1}(t') - 2E_n(t')] \tag{3}$$

for all n.

We return to the lattice with one fixed transition rate . For sites which are not connected to bonds of the embedded cluster, the probability $P_n(t)$ of finding particle at site n and time t satisifies the same master equation as $E_n(t)$, equation (3).

However, for sites within or contiguous with the embedded cluster, the transition rates are random functions and the system is described by the equation below,

$$\begin{aligned}\frac{\partial P_n}{\partial t} &= \int_0^t dt'\Gamma(t-t')(1-\delta_{n,1})[-P_n(t')+P_{n-1}(t')] \\ &+ \delta_{n,1}\Gamma'[P_{n-1}(t')-P_n(t')] \\ &+ \int_0^t dt'\Gamma(t-t')(1-\delta_{n,0}[P_{n+1}(t')-P_n(t')] \\ &+ \delta_{n,0}\Gamma'[P_{n+1}-P_n(t')].\end{aligned} \tag{4}$$

Laplace transformation yields

$$\begin{aligned}s\tilde{P}_n(s) &= P_n(t=0)-\Gamma(s)[2\tilde{P}_n(s)-\tilde{P}_{n+1}(s)-\tilde{P}_{n-1}(s)] \\ &+[\Gamma(s)-\Gamma'](\delta_{n,1}-\delta_{n,0})[\tilde{P}_1(s)-\tilde{P}_0(s)].\end{aligned} \tag{5}$$

Fourier transformation,

$$P(k)=\sum_n e^{-ikan}P_n \tag{6}$$

leads to

$$[s+2\Gamma(s)(1-coska)]\ \tilde{P}\ (k,s)=1+(e^{-ika}-1)[\Gamma(s)-\Gamma'][\tilde{P}_1\ (s)-\tilde{P}_0\ (s)]. \tag{7}$$

The equation for the effective medium after Fourier and Laplace transformation of equation (3) is

$$[s+2\Gamma(s)(1-coska)]\ \tilde{E}\ (k,s)=1. \tag{8}$$

Comparing (7) and (8) we arrive at

$$\tilde{P}\ (k,s)=\tilde{E}\ (k,s)+\ \tilde{E}\ (k,s)(e^{-ika}-1)[\Gamma(s)-\Gamma'][\tilde{P}_1\ (s)-\tilde{P}_0\ (s)]$$

The inverse Fourier transformation of (8) is given by

$$\begin{aligned}\tilde{E}_n\ (s) &= \frac{1}{N}\sum_k \frac{e^{inka}}{s+2\Gamma(s)(1-coska)} \\ \tilde{E}_n\ (s) &= \frac{1}{\pi}\int_0^\pi dk \frac{cosnk}{s+2\Gamma(s)(1-coska)}.\end{aligned} \tag{9}$$

We can see from this that

$$\tilde{E}_n(s) = \tilde{E}_{-n}(s) \tag{10}$$

and utilizing this the following equations can be obtained

$$\begin{aligned} \tilde{P}_0(s) &= \tilde{E}_0 + (\tilde{E}_1 - \tilde{E}_0)[\Gamma(s) - \Gamma'][\tilde{P}_1(s) - \tilde{P}_0(s)] \\ \tilde{P}_1(s) &= \tilde{E}_1 + (\tilde{E}_0 - \tilde{E}_1)[\Gamma(s) - \Gamma'][\tilde{P}_1(s) - \tilde{P}_0(s)]. \end{aligned} \tag{11}$$

Adding and subtracting these two equations results in the following equations, respectively,

$$\begin{aligned} \tilde{P}_0 + \tilde{P}_1 &= \tilde{E}_0 + \tilde{E}_1 \\ \tilde{P}_0 - \tilde{P}_1 &= \tilde{E}_0 - \tilde{E}_1 + 2[\tilde{\Gamma}(s) - \Gamma'](\tilde{E}_1 - \tilde{E}_0)(\tilde{P}_1 - \tilde{P}_0). \end{aligned} \tag{12}$$

Combining the above two equations and solving for $\tilde{P}_0$ one obtains

$$\tilde{P}_0(s) = \tilde{E}_0(s) + \frac{(\tilde{E}_1 - \tilde{E}_0)^2[\tilde{\Gamma}(s) - \Gamma']}{1 + 2(\tilde{E}_1 - \tilde{E}_0)[\tilde{\Gamma}(s) - \Gamma']} \tag{13}$$

We now require the average over the distribution of the random bonds that are embedded into the effective–medium, gives the same result as the effective–medium itself,

$$\{\tilde{P}_0(s)\} = \tilde{E}_0(s) \tag{14}$$

Averaging equation (13) over the distribution of Γ' and using (14) gives

$$\left\{ \frac{(\tilde{E}_1 - \tilde{E}_0)^2[\tilde{\Gamma}(s) - \Gamma']}{1 + 2(\tilde{E}_1 - \tilde{E}_0)[\tilde{\Gamma}(s) - \Gamma']} \right\} = 0 \tag{15}$$

Solving the master equation for $E_0(t)$, the probability of a particle to be at point '0' at time t, and making the Laplace transform, we get

$$\tilde{E}_1(s) - \tilde{E}_0(s) = \frac{s\,\tilde{E}_0(s) - 1}{2\,\tilde{\Gamma}(s)} \tag{16}$$

Using equation (16) in (15) and utilizing the fact that $(\widetilde{E}_1 - \widetilde{E}_0)^2$ is not stochastic to omit it from the average we obtain

$$\left\{ \frac{\widetilde{\Gamma}(s) - \Gamma'}{1 + \frac{sE_0(s)-1}{\widetilde{\Gamma}(s)}[\widetilde{\Gamma}(s) - \Gamma']} \right\}_{\rho(\Gamma')} = 0 \tag{17}$$

In the lim $s \to 0$, i.e. in the long time limit $s\ \widetilde{E}_0(s) \to 0$. The detailed mathematical proof is shown in Appendix A. Hence, the one dimensional self consistency condition is now reduced to,

$$\left\{ \frac{\widetilde{\Gamma}(s \to 0) - \Gamma'}{\Gamma'} \right\}_{\rho(\Gamma')} = 0 \tag{18}$$

This relation can be simplified to

$$\widetilde{\Gamma}(s \to 0) = \left\{ \frac{1}{\Gamma'} \right\}^{-1} \tag{19}$$

The average is now taken over the random transition rate appearing in the embeded cluster.

2.2 Square Lattice $(d = 2)$

As for the one-dimensional lattice, the one stochastic barrier is chosen randomly and placed on the square lattice, as in fig. (3). The probability $E_{mn}(t)$ of finding a particle at m and n at time t when the lattice consists of only effective-medium rates satisfies master equation where m is counted in x-direction and n in the y-direction.

$$\begin{aligned} \frac{\partial E_{mn}(t)}{\partial t} &= \int_0^t dt' \Gamma(t-t') \left[-2E_{mn}(t') + E_{mn+1}(t') + E(t') \right] \\ &+ \int_0^t dt' \Gamma(t-t') \left[E_{m+1n}(t') + E_{m-1n}(t') - 2E_{mn}(t') \right]. \end{aligned} \tag{20}$$

With one stochastic barrier included, the master equation for the probability $P_{mn}(t)$ is written:

$$
\begin{aligned}
\frac{\partial}{\partial t} P_{mn}(t) &= \int_0^t dt' \Gamma(t-t')(1-\delta_{m0}\delta_{n0})\,[P_{m+1n}(t') - P_{mn}(t')] \qquad (21)\\
&+ \delta_{m0}\delta_{n0}\Gamma'[-P_{00}(t) + P_{10}(t)]\\
&+ \int_0^t dt' \Gamma(t-t')\,(1-\delta_{m1}\delta_{n0})\,[-P_{mn}(t') + P_{m-1n}(t')]\\
&+ \delta_{m1}\delta_{n0}\Gamma'[P_{00}(t) - P_{10}(t)]\\
&+ \int_0^t dt' \Gamma(t-t')\,[P_{mn+1}(t') - P_{mn}(t')]\\
&+ \int_0^t dt' \Gamma(t-t')\,[P_{mn-1}(t') - P_{mn}(t')].
\end{aligned}
$$

Taking the Laplace transform, one has

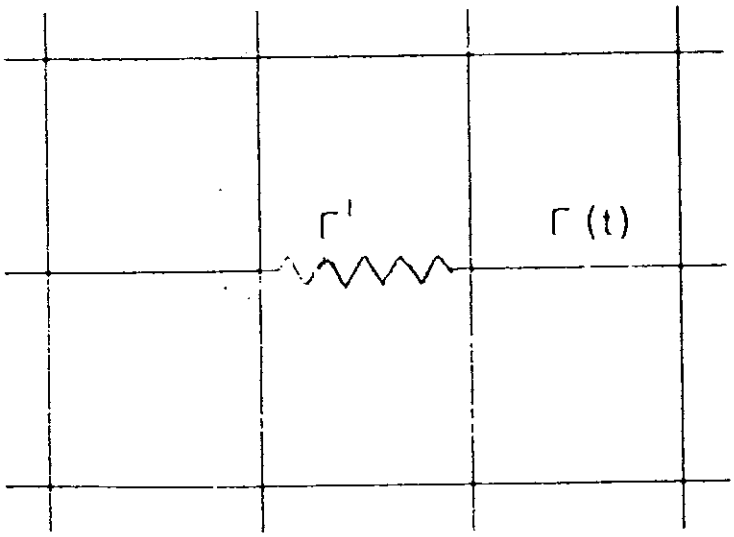

Figure 3: Two dimensional square lattice model with one stochastic barrier embedded in it.

$$
\begin{aligned}
s\,\tilde{P}_{mn}(s) &= P_{mn}(t=0) \qquad (22)\\
&- \tilde{\Gamma}(s)[4\,\tilde{P}_{mn} - \tilde{P}_{m+1n} - \tilde{P}_{mn+1} - \tilde{P}_{mn-1}]\\
&+ [\tilde{\Gamma}(s) - \Gamma'][\tilde{P}_{00}(s) - \tilde{P}_{10}(s)]\,[\delta_{m0}\delta_{n0} - \delta_{m1}\delta_{n0}].
\end{aligned}
$$

Implementing the Fourier transformation, where

$$\mathcal{F}[P_{mn}] = P(k_1, k_2) = \sum_{m,n} \exp[-i(k_1 m + k_2 n)] P_{mn} \tag{23}$$

and 'a' the lattice constant is taken to be $a = 1$, yields

$$\begin{aligned} &[s + 2\,\tilde{\Gamma}\,(s)(2 - cosk_1 - cosk_2)]\;\tilde{P}\,(k, s) \\ &= 1 + [\tilde{\Gamma}\,(s) - \Gamma'][\tilde{P}_{00}\,(s) - \tilde{P}_{10}\,(s)][1 - e^{-ik_1}]. \end{aligned} \tag{24}$$

The equation for the effective medium (without stochastic barrier Γ') after Laplace and Fourier transform is,

$$[s + 2\Gamma(s)\,(2 - cosk_1 - cosk_2)]\;\tilde{E}\,(\underline{k}, s) = 1. \tag{25}$$

Combining equation (24) and (25) gives

$$\tilde{P}\,(k, s) = \tilde{E}\,(k, s) + \tilde{E}\,(k, s)\,(e^{-ik_1} - 1)\,[\tilde{\Gamma}\,(s) - \Gamma'][\tilde{P}_{10}\,(s) - \tilde{P}_{00}\,(s)] \tag{26}$$

The inverse Fourier transform of equation (25) is

$$\begin{aligned} \tilde{E}_{mn} &= \frac{1}{N} \sum_{k_1 k_2} \frac{\exp[i(k_1 m + k_2 n)]}{s + 2\,\tilde{\Gamma}\,(s)\,(2 - cosk_1 - cosk_2)} \\ &= \frac{1}{(2\pi)^2} \int_{-\pi}^{\pi} \int_{-\pi}^{\pi} dk_1\, dk_2 \frac{\exp[i(k_1 m + k_2 n)]}{s + 2\,\tilde{\Gamma}\,(s)\,(2 - cosk_1 - cosk_2)} \\ \tilde{E}_{mn} &= \frac{1}{\pi^2} \int_{-\pi}^{\pi} \int_{-\pi}^{\pi} dk_1\, dk_2 \frac{cos(mk_1)cos(nk_2)}{s + 2\,\tilde{\Gamma}\,(s)(2 - cosk_1 - cosk_2)} \end{aligned} \tag{27}$$

We only need $\tilde{E}_{00}, \tilde{E}_{10}$, where the stochastic barrier is embedded. The following symmetry holds:

$$E_{-mn} = E_{mn} = E_{m-n}$$

Using equation (26) one arrives at

$$\begin{aligned} \tilde{P}_{00} &= \tilde{E}_{00} + (\tilde{E}_{10} - \tilde{E}_{00})\,[\tilde{\Gamma}\,(s) - \Gamma'][\tilde{P}_{10} - \tilde{P}_{00}] \\ \tilde{P}_{10} &= \tilde{E}_{10} + (\tilde{E}_{00} - \tilde{E}_{10})\,[\tilde{\Gamma}\,(s) - \Gamma'][\tilde{P}_{10} - \tilde{P}_{00}]. \end{aligned} \tag{28}$$

Similar to the one dimensional derivation, combing these two equations, one arrives at an equivalent expression

$$\tilde{P}_{00}(s) = \tilde{E}_{00}(s) + \frac{[\tilde{E}_{10}(s) - \tilde{E}_{00}(s)]^2 [\tilde{\Gamma}(s) - \Gamma']}{1 + 2[\tilde{E}_{10}(s) - \tilde{E}_{00}(s)][\tilde{\Gamma}(s) - \Gamma']}. \tag{29}$$

As in one dimension, it is required that the average $\{P_{00}(s)\}$is identical to the effective–medium probability $E_{00}(s)$, cf(14). Averaging over the distribution of Γ', one obtains

$$\left\{ \frac{\tilde{\Gamma}(s) - \Gamma'}{1 + 2[\tilde{E}_{10}(s) - \tilde{E}_{00}(s)][\tilde{\Gamma}(s) - \Gamma']} \right\}_{\rho(\Gamma')} = 0 \tag{30}$$

$\tilde{E}_{10} - \tilde{E}_{00}$ can be expressed through $\tilde{E}_{00}(s)$, similar to equation (16),

$$\tilde{E}_{10}(s) - \tilde{E}_{00}(s) = s \frac{\tilde{E}_{00}(s) - 1}{4\,\tilde{\Gamma}(s)} \tag{31}$$

Substitution into equation (30) gives

$$\left\{ \frac{\tilde{\Gamma}(s) - \Gamma'}{\tilde{\Gamma}(s) + \Gamma' + s\,\tilde{E}_{00}(s)[\tilde{\Gamma}(s) - \Gamma']} \right\}_{\rho(\Gamma')} = 0 \tag{32}$$

This reduces to the following equation when $lim_{s \to 0}$, $s\ \tilde{E}_{00}(s) \to 0$ is taken into account, see Appendix B.

$$\left\{ \frac{\tilde{\Gamma}(s \to 0) - \Gamma'}{\tilde{\Gamma}(s \to 0) + \Gamma'} \right\}_{\rho(\Gamma)} \tag{33}$$

This is the self–consistency condition we utilize in calculating the diffusion coefficient for our model. A more general expression for the self consistency condition for one stochastic barrier can be obtained for arbitrary dimension. Consider either equation (30) or (15) and from the form of the expression for $\dot{E}_0$ and $\dot{E}_{00}$ one can surmise the self consistency condition for arbitrary dimension:

$$\left\{ \frac{\tilde{\Gamma}(s \to 0) - \Gamma'}{(z-2)\,\tilde{\Gamma}(s \to 0) + 2\Gamma'} \right\}_{\rho(\Gamma')} = 0 \tag{34}$$

where z is the coordination number and $z = 2d$ for simple lattices, d is dimension.

$$\left\{ \frac{\tilde{\Gamma}(s \to 0) - \Gamma'}{d\tilde{\Gamma}(s \to 0) - [\tilde{\Gamma}(s \to 0) - \Gamma']} \right\}_{\rho(\Gamma')} = 0 \qquad (35)$$

2.3 The Mean-Square Displacement

One of the most important physical parameters describing random walk is the mean-square displacement $\{R(t)^2\}$ covered by the random walker after having stepped t steps or (equivalently, after time t). The long and short time behaviour of the mean-square displacement is now known exactly for the one dimensional disordered lattice, and in a good approximation for higher dimensions /14,19/. In our simulation we monitored this moment to determine the diffusion coefficient in the long time limit. Here we try to show how the long time behaviour of the mean square displacement is obtained from the result of the Effective-Medium Theory, $\tilde{\Gamma}(s \to 0)$. For small k, that is $k \to 0$, P(k, s) of equation (7) for one dimension is given by

$$\tilde{P}(k,s) = \frac{1}{s + 2\tilde{\Gamma}(s)\frac{k^2}{2}}$$

$$\tilde{P}(k,s) = \frac{1}{s} \frac{1}{1 + \frac{2\tilde{\Gamma}(s)}{s}\frac{k}{2}} \qquad (36)$$

where, to get the above expression the expansion of cosk for small k is used. Expanding equation (36) in Taylor series we get

$$\tilde{P}(k,s) = \frac{1}{s}\left[1 - \frac{2\tilde{\Gamma}(s)}{s}\frac{k^2}{2} \right] \qquad (37)$$

Considering the Fourier transform of $\tilde{P}$(k, s)

$$\tilde{P}(k,s) = \frac{1}{N}\sum_{k} \exp^{-ikx}\tilde{P}(x,s) \qquad (38)$$

the expression for the mean-square displacement can be derived, which is

$$\{X^2\} = \left[-\frac{\partial^2 \tilde{P}}{\partial k^2} \right]_{k=0} \qquad (39)$$

Applying this on equation (37) gives, in the laplace domain

$$\left\{X^2\right\} = \frac{2\ \tilde{\Gamma}\ (s)}{s^2}. \tag{40}$$

Expansion of $\tilde{\Gamma}\ (s)$ for small s is assumed to be

$$\tilde{\Gamma}\ (s) = \Gamma s \to 0 \left[1 + \theta_1 s^{\frac{1}{2}} + \theta_2 s + \theta_3 s^{\frac{3}{2}} + \cdots\right]$$

and hence equation(40) becomes

$$\{X^2\} = 2\Gamma s \to 0 \left[\frac{1}{s^2} + \frac{\theta_1}{s^{\frac{3}{2}}} + \frac{\theta_2}{s} + \frac{\theta_3}{s^{\frac{1}{2}}} + \cdots\right]. \tag{41}$$

Taking the inverse Laplace transform the time domain, behaviour for large t of the mean–square displacement is found,

$$\{X^2\}(t) = 2\Gamma(s \to 0)\left[t + 2\theta_1 \left(\frac{t}{\pi}\right)^{\frac{1}{2}} + \theta_2 + \frac{\theta_3 t}{\pi^{\frac{1}{2}}} + \cdots\right]. \tag{42}$$

θ_1, θ_2 and θ_3 are the correction parameters of the mean–square displacement for long times. They can be calculated by putting back the expression for $\tilde{\Gamma}\ (s)$ into the self consistency condition and letting terms of the same order in s vanish. These correction values and diffusion coefficient for two dimensional lattice with its are given in appendix C.

The limit of $\tilde{\Gamma}\ (s \to 0)$ is derived from the self consistency condition of the effective–medium theory and we will call it Γ_{eff} in the remainder. The asymptotic behaviour of the mean–squarer displacement in $d = 1$ is usually written as

$$\lim_{t\to\infty} \left\{X^2(t)\right\} = 2\ D_0\ t. \tag{43}$$

Comparing (43) with (42) we find

$$D_0 = \Gamma(s \to 0) = \Gamma_{eff}. \tag{44}$$

The derivation of this section are easily extended to arbitrary dimensions, except that the form of the small–s expansion of $\tilde{\Gamma}\ (s)$ depends on dimensionality /14/. The

expansion for the mean-square displacement on d dimensions for the hypercubic lattices is

$$\lim_{t\to\infty}\left\{X^2(t)\right\} = 2\,d\,\Gamma_{eff}\,t \tag{45}$$

It is found that equation (45) is valid for arbitrary dimensions.

3 The Random Barrier Model

In the present investigation the random barriers have been defined by transition rates. As it is stated in the introduction section, disorder is introduced in this model by considering an inhomogeneous distribution of symmetric transition rates from one site to the next, that is the transition rate for a jump from a site to a particular neighbor is the same as the rate from that neighbor to the original site or in other words once a forward jump is made in a particular direction, then the backward jump should carry the same probability as the forward jump.

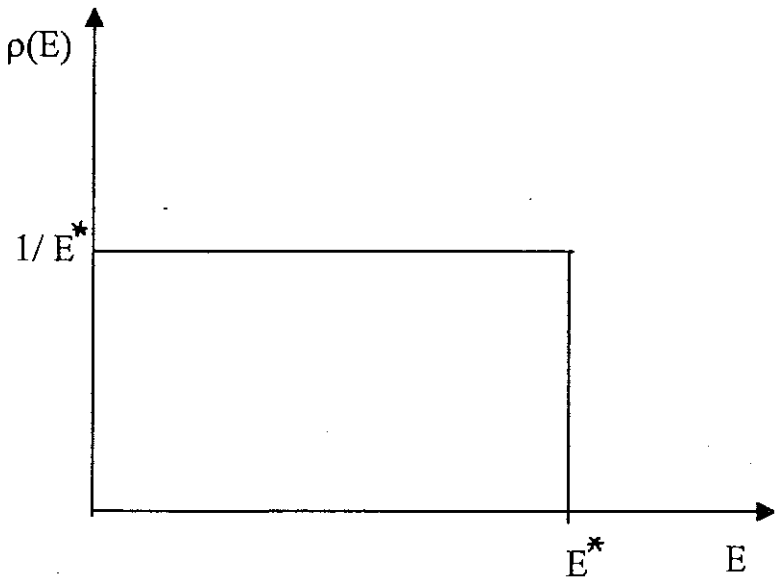

Figure 4: Uniform distribution of the activation energy E

We now relate the transition rates to thermally activated processes that are governed by Boltzmann statistics. In perfectly ordered crystals one could assume the existence of a single activation energy. Spatial disorder in amorphous systems, as it is in our case should imply the activation energy E being a random variable, subject to some probability distribution ν(E). ν(E) is a uniform distribution depicted in fig.4.

The normalized distribution is expressed as

$$\nu(E) = \begin{cases} \frac{1}{E^*} & 0 \leq E \leq E^* \\ 0 & otherwise \end{cases} \tag{46}$$

The transition rate Γ between two neighbor sites is related to the randomly selected energy E by means of the Arrhenius law

$$\Gamma = \Gamma_0 \exp\left(-\frac{E}{K_B T}\right), \quad E > 0 \tag{47}$$

where Γ_0 is the maximum possible transition rate between neighboring sites at equilibrium and it is taken to be $\frac{1}{2d}$, where d is the lattice dimension through out this work. The ratio $\frac{E}{K_B T} = \frac{1}{\alpha}$ is a controlling parameter that is to be carefully investigated here. E is the activation energy, K_B is the Boltzmann constant and T is temperature. You see from the distribution, if we randomly select the activation energy near E^*, the particle hardly jumps. It means many jumps will be performed there. Therefore the contribution of such particles with a large barrier in front towards diffusivity would be negligibly small. On the other hand if energies closer to the origin are randomly selected; many, many particles would be able to jump farther so as to contribute to the conductivity of the system. This is possible provided the temperature is not very small.

What we implement in the simulation is: we define ϵ which is a random number between 0 and 1 as $\epsilon = \frac{E}{E^*}$. E then becomes $E = \epsilon E^*$. Substituting this into the Arrenhius law we have

$$\Gamma = \Gamma_0 \exp\left(\frac{-\epsilon E^*}{K_B T}\right)$$

or

$$\Gamma = \Gamma_0 \exp\left(\frac{-\epsilon}{\alpha}\right).$$

From the uniform random number generator we get ϵ; and α is at our disposal so the corresponding transition rate is known. Γ_0 which we call the maximum transition

rate has the inherent property of diffusing particle in it. The random barriers are basically built according to the random numbers which are chosen from the uniform distribution we are considering.

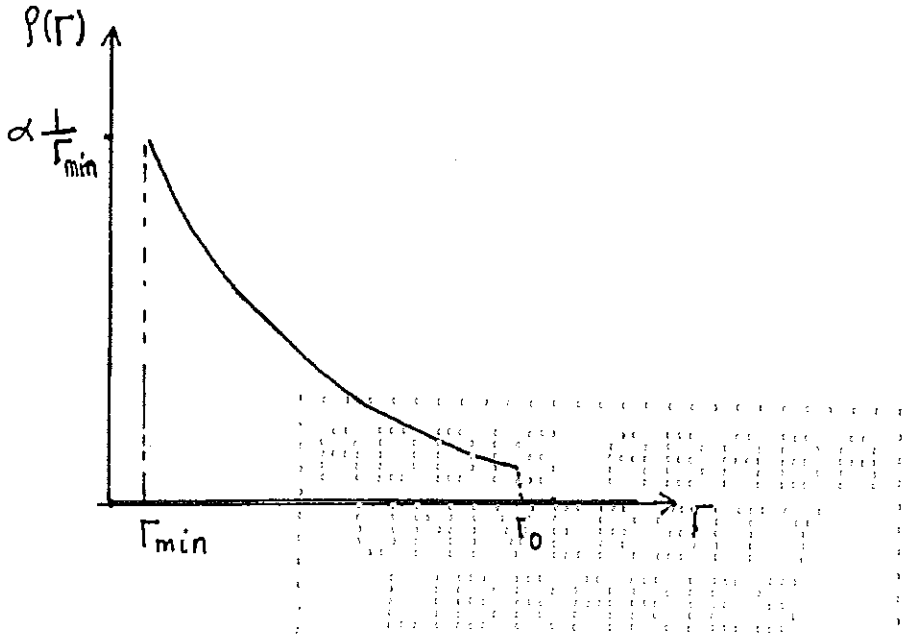

Figure 5: An equivalent distribution for the transition rates.

One can also make a transformation to find the distribution of transition rates $\rho(\Gamma)$

$$\rho(\Gamma)d\Gamma = \nu(E(\Gamma))dE$$

$$\rho(\Gamma) = \nu(E(\Gamma))\left|\frac{dE}{d\Gamma}\right|$$

Considering equation (47) and differentiating yields

$$\rho(\Gamma) = \frac{K_B T}{E^*}\frac{1}{\Gamma}. \tag{48}$$

Including the range of validity the above equation is

$$\rho(\Gamma) = \begin{cases} \alpha\frac{1}{\Gamma} & \Gamma_{min} \leq \Gamma \leq \Gamma_0 \\ 0 & otherwise \end{cases} \tag{49}$$

and it is plotted in fig. 5. E^* is the maximum activation energy the particle should surmount, and $\Gamma_{min} = \Gamma_0 \exp\left(-\frac{1}{\alpha}\right)$.

3.1 Derivation of Diffusion Coefficient from Self Consistency Condition

Here we are going to solve the self-consistency condition for the particular distribution of the model, for one dimension, two dimensions and three dimensions respectively. The self-consistency condition as it is derived in section 2 is

$$\left\{ \frac{\Gamma_{eff} - \Gamma}{d\Gamma_{eff} - (\Gamma_{eff} - \Gamma)} \right\}_{\rho(\Gamma)} = 0 \tag{50}$$

3.1.1 One Dimension

substituting $d = 1$, the self consistensy condition above reduces to

$$\left\{ \frac{\Gamma_{eff} - \Gamma}{\Gamma} \right\}_{\rho(\Gamma)} = 0 \tag{51}$$

solving for Γ_{eff} yields

$$\Gamma_{eff} = \left\{ \frac{1}{\Gamma} \right\}^{-1} \tag{52}$$

Γ_{eff} coincides with the exact result for the diffusion coefficient of the RBM in one dimension /14,19/ . So, for our continous distribution of the transition rate and activation energy, the average value $\left\{ \frac{1}{\Gamma} \right\}$ can be calculated as follows to get the expression for the diffusion coefficient.

$$\left\{ \frac{1}{\Gamma} \right\} = \int_{\Gamma_{min}}^{\Gamma_{max}} d\Gamma \rho(\Gamma) \frac{1}{\Gamma} = \int_0^{E^*} dE\, \nu(E) \frac{1}{\Gamma(E)} \tag{53}$$

Using equation (46) and (47), the above equation becomes:

$$\begin{aligned} \left\{ \frac{1}{\Gamma} \right\} &= \int_0^{E^*} dE \frac{1}{\Gamma_0 E^*} \exp\left(\frac{E}{K_B T}\right) \\ &= \frac{K_B T}{\Gamma_0 E^*} \exp \frac{E}{K_B T} \Big|_0^{E^*} \\ \left\{ \frac{1}{\Gamma} \right\} &= \frac{K_B T}{\Gamma_0 E^*} \left\{ \exp \frac{E^*}{K_B T} - 1 \right\}. \end{aligned}$$

The expression for the diffusion coefficient can be obtained by taking the inverse of equation above

$$\Gamma_{eff} = \left\{\frac{1}{\Gamma}\right\}^{-1} \tag{54}$$

$$\Gamma_{eff} = \frac{\Gamma_0 E^*}{K_B T}\left\{\frac{1}{\exp\frac{E^*}{K_B T} - 1}\right\}$$

Considering the two extreme cases, the diffusion coefficient for one dimensional lattices reduces as follows

$$\Gamma_{eff} = \begin{cases} \Gamma_0 & \text{if } E^* \ll K_B T \\ \frac{\Gamma_0 E^*}{K_B T}\exp(-\frac{E^*}{K_B T}) & \text{if } E^* \gg K_B T \end{cases} \tag{55}$$

This result means, that at very high temperatures the barriers do not play a role at all and the diffusion coefficient is given by, Γ_0, while at very low temperature the diffusion coefficient is determined by the highest possible barriers.

3.1.2 Two Dimensions

The self-consistency condition for the already described continous distribution of the transition rate is

$$\int_{\Gamma_{min}}^{\Gamma_{max}} \rho(\Gamma)\, d\Gamma\, \frac{\Gamma_{eff} - \Gamma}{\Gamma_{eff} + \Gamma} = 0 \tag{56}$$

where Γ_{max} and Γ_{min} are Γ_0 and $\Gamma_0 \exp\left[-(\frac{E^*}{K_B T})\right]$ respectively. The expression for the distribution of the transition rates is the same as used for the one- dimensional case, i.e. equation (48). Substituting this expression into the above self consistency condition for two dimensional lattices, we get

$$\frac{K_B T}{E^*}\int_{\Gamma_{min}}^{\Gamma_0} d\Gamma\, \frac{1}{\Gamma}\, \frac{\Gamma_{eff} - \Gamma}{\Gamma_{eff} + \Gamma} = 0. \tag{57}$$

Dividing each term in the numerator by the denominator it becomes

$$\int_{\Gamma_{min}}^{\Gamma_0} \left(\frac{\Gamma_{eff}}{\Gamma(\Gamma_{eff} + \Gamma)} - \frac{1}{\Gamma_{eff} + \Gamma}\right) d\Gamma = 0. \tag{58}$$

To integrate this we proceed as follows, expanding the first term, that is

$$\frac{\Gamma_{eff}}{\Gamma(\Gamma_{eff}+\Gamma)} = \Gamma_{eff}\left(\frac{a}{\Gamma}+\frac{b}{\Gamma_{eff}+\Gamma}\right) \tag{59}$$

making some rearrangments and solving for a and b gives

$$a = \frac{1}{\Gamma_{eff}}$$

$$b = -\frac{1}{\Gamma_{eff}}.$$

Substituting the values of a and b into equation (58) gives

$$\begin{aligned}
\int_{\Gamma_{min}}^{\Gamma_0}\left(\frac{1}{\Gamma}-\frac{2}{\Gamma_{eff}+\Gamma}\right)d\Gamma &= 0 \\
\left[\ln\frac{\Gamma}{(\Gamma_{eff}+\Gamma)^2}\right]_{\Gamma_{min}}^{\Gamma_0} &= 0 \\
\ln\frac{\Gamma_0}{\Gamma_{min}}\left(\frac{\Gamma_{eff}+\Gamma_{min}}{\Gamma_{eff}+\Gamma_0}\right)^2 &= 0 \\
\frac{\Gamma_0}{\Gamma_{min}} &= \left(\frac{\Gamma_{eff}+\Gamma_0}{\Gamma_{eff}+\Gamma_{min}}\right)^2.
\end{aligned}$$

Evaluating the limits of integral and using the expression for Γ_{min} we arrive at the required result, the expression for the diffusion coefficient Γ_{eff} in two-dimensional lattices.

$$\Gamma_{eff} = \Gamma_0 \exp -\frac{E^*}{2K_BT} \tag{60}$$

3.1.3 Three Dimension

As for the other lower dimensions the diffusion coefficient for particles in three-dimensional lattices can be derived from the self consistency condition, where $d = 3$ is to be substituted first. The self consistency condition is

$$\left\{\frac{\Gamma_{eff}-\Gamma}{2\Gamma_{eff}+\Gamma}\right\}_{p(\Gamma)} = 0 \tag{61}$$

$$\int_{\Gamma min}^{\Gamma_0} \rho(\Gamma)\, d\Gamma\, \frac{\Gamma_{eff} - \Gamma}{2\,\Gamma_{eff} + \Gamma} \;=\; 0$$

Using the same method as the two dimensions and solving the integral we arrive at the expression for the diffusion coefficient

$$\Gamma_{eff} = \frac{\Gamma_0}{2}\left[\frac{1 - \exp(-\frac{2E^*}{3K_BT})}{\exp\frac{E^*}{3K_BT} - 1}\right] \tag{62}$$

This expression reduces for $\alpha \to 0$ to

$$\Gamma_{eff} = \frac{\Gamma_0}{2}\,\exp(-\frac{1}{3\alpha}) \tag{63}$$

The result for any dimension $d \geq 2$ is then

$$\Gamma_{eff} = \frac{\Gamma_0}{d-1} \cdot \frac{1 - \exp\frac{(1-d)}{d\alpha}}{\exp(\frac{1}{d\alpha}) - 1} \tag{64}$$

extension of the result to other intervals of the energy are also possible. For fixed dimension d and small parameter α the expression reduces to

$$\Gamma_{eff}\ \alpha \xrightarrow{} 0\ \frac{\Gamma_0}{d-1}\exp(-\frac{1}{d\alpha}) \tag{65}$$

The diffusion coefficients, for small values of α is found to be in the following order, smallest in one larger in two and largest in three dimension. The physical reason is, at lower temprature the harriers look high enough to prevent the motion of particles. In higher dimensions there are multiple paths where particle can percolate through, hence the diffusion coefficient is not as much reduced than in one dimension.

3.2 Mobility When Force is Applied

During a biased random walk the particle drifts in a preferential direction. The field causing the biased drift could be local, that is restricted to a few lattice sites, or it could be global, extending over the whole lattice. An applied static electric field of the sample can be used to induce a drift in a preferential direction on the whole

lattice. whereas, local charge centers or defects in the lattice can cause a local drift in to a region of lower potential energy. These random walks can be important in understanding significant physical properties of materials /21,22/. Internal structures, such as atomic impurities, dislocations or vacancies can locally distort the lattice over several lattice sites. The extended internal structures cause a local drift as the particle falls into and climbs out of the distorted regions.

In our work the force is assumed to have global effect, and considering the linear response of the particle to the applied force, we try to determine the mean displacement which is obviously different from zero; because particles are allowed to move to a more preferential direction along the direction of the applied field. The mean displacement is related to the diffusion coefficient via Einstein relation. Suppose that static electric field is applied along the positive X - direction on one dimensional lattice considered below. The selection of the bias direction is arbitrary and has no effect on the final result. We can see from fig.6b the lattice structure is inclined along the direction of the force to allow more particles to easily slide, whereas the barrier increases against the direction of bias allowing few particles to diffuse.

To derive the bias factor B and the mean displacement, consider the transition rate from site i to site $i + 1$ as it is depicted in fig.6a with no bias. Now for the biased case, the transition rate becomes

$$\Gamma_{i\to i+1} = \Gamma_0 \exp -\left(\frac{E_i - \frac{Fa}{2}}{K_B T}\right) \tag{66}$$

$$= \Gamma_0 \exp -\left(\frac{E_i}{K_B T}\right) \exp \frac{Fa}{2K_B T}$$

$$\Gamma_{i\to i+1} = \Gamma_{i\to i+1}^{nobias} B \tag{67}$$

where

$$B = \exp \frac{Fa}{2k_B T} \tag{68}$$

and F and a are the magnitude of the force applied and are the lattice constant respectively. The lattice constant a is taken to be 1 through out the calculation. The factor B is due to the relative changes in the potential barrier as seen from the initial site, as is shown in fig.6b. This factor is the bias, which we utilize in our simulations to favour the transitions of particles along a specific direction.

For the other direction of motion , the transition rates are shown below

$$\begin{aligned} \Gamma_{i\leftarrow i+1} &= \Gamma_0 \exp -(\frac{E_i + \frac{F}{2}}{K_B T}) \\ \Gamma_{i\leftarrow i+1} &= \Gamma^{no\ bias}_{i\rightarrow i+1}\ B^{-1} \end{aligned} \tag{69}$$

and you see that the motion is retarded by a factor of $\frac{1}{B}$. For F very small, as it is already assumed , the expression for B is expanded to give :

$$\begin{aligned} B &= 1 + \frac{F}{2K_B T} \\ B - 1 &= \frac{F}{2K_B T}. \end{aligned} \tag{70}$$

When a force acts on the particles, they move with a velocity V, and the mean displacement will be proportional to time,

$$\{X\} = Vt. \tag{71}$$

The velocity is related in linear response to the force by the mobility μ,

$$V = \mu\ F. \tag{72}$$

Using the Einstein relation between mobility and diffusion coefficient, $\mu = \frac{\Gamma_{eff}}{K_B T}$, we obtain

$$\{X\} = 2\Gamma_{eff} \left(\frac{F}{2K_B T}\right) t \tag{73}$$

The same result is obtained in two and three dimensions, when the bias is applied in X–direction only . Formula (71) allows to determine Γ_{eff} (the diffusion coefficient)

from simulations of the mean displacement, when a bias $B = 1 + F/2K_B T$ is applied. In our simulation, B is taken to be 1.05. It should be noted that (71) or (73) are valid on the long - time limit, and there may transient effects present at short times.

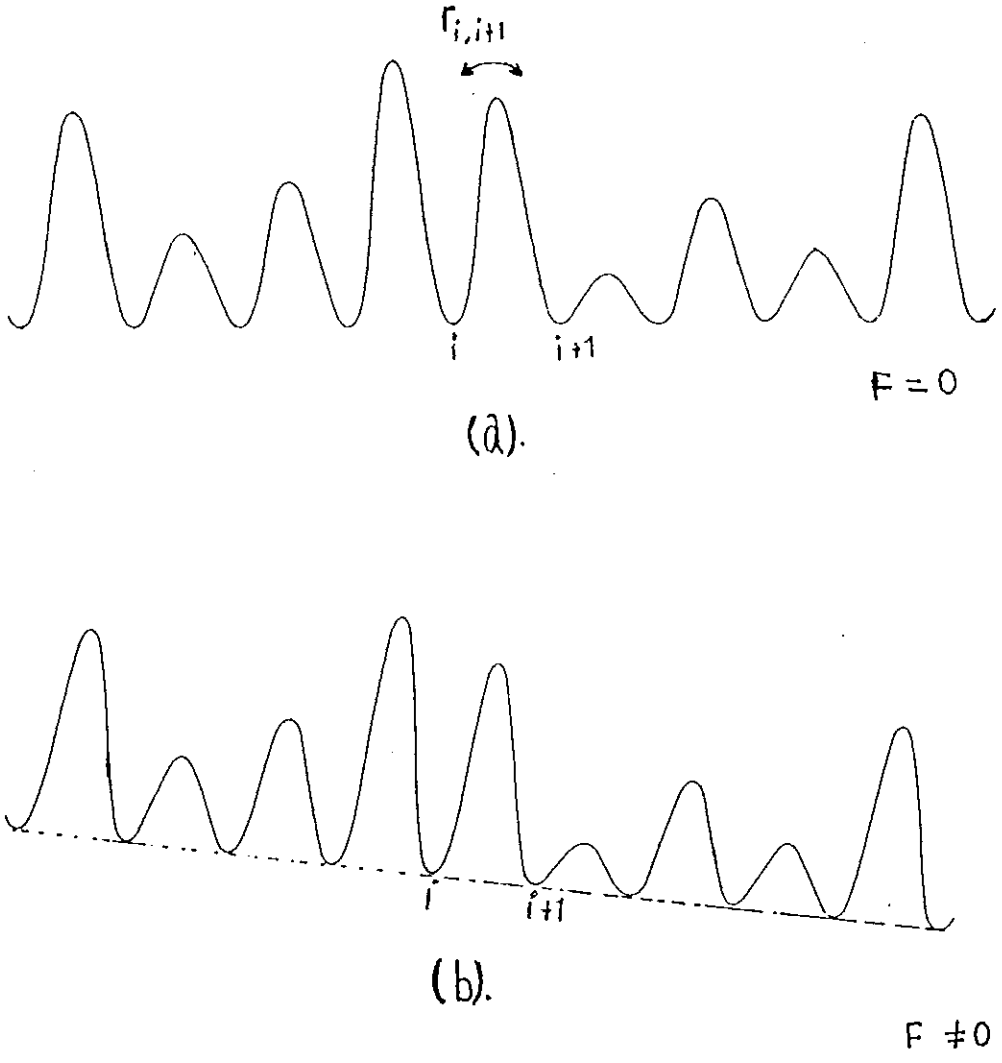

Figure 6: Schematic representation of biased system for one dimension case. (a) is without bias and (b) is with bias in the positive X - direction.

4 Estimate of Effective Hopping Rate from Percolation Theory

In this section we will describe an alternative estimate for the effective hopping rate in the random-barrier model. The effective-medium theory provides approximation results for the effective hopping rate in two and three dimensions, and one does not know the accuracy of this approximation. At low temperatures one has very wide distribution of transition rates. It was suspected /23,24/ that the EMT might not be good in such situations. Hence an alternative picture was developed which will be described below. It is one of the aims of the present work to examine whether the EMT or the alternative estimate are on better agreement with the simlations.

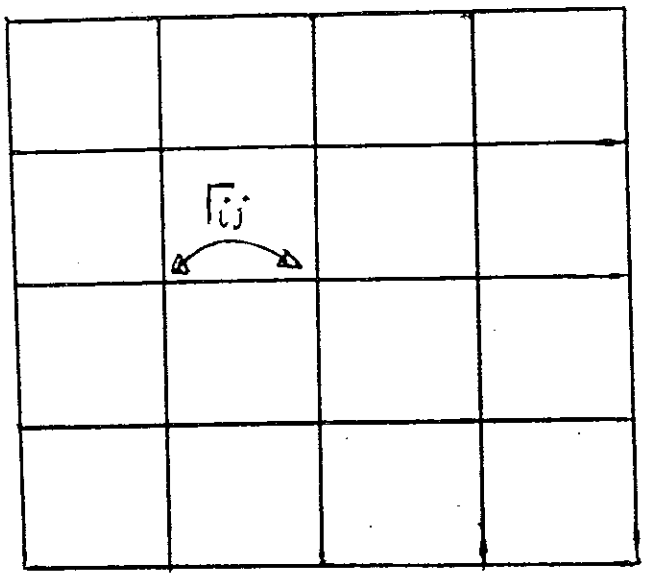

Figure 7: Two dimensional square lattice with every bond being inactive.

Consider a d-dimensional lattice . Assign independent symmetric random hopping rates between neighbouring sites Γ_{ij} fig.(7), taken from a common distribution $\rho(\Gamma)$. Consider all hopping rates to be inactive. Take the largest rate out of the set

$\{\Gamma_{ij}\}$and make it active, take the next largest rate etc. After a while, we have isolated, active hopping rates, see fig.(8). Continue until there is a continous path from one boundary of the large lattice to the opposite boundary fig.(9). This happens

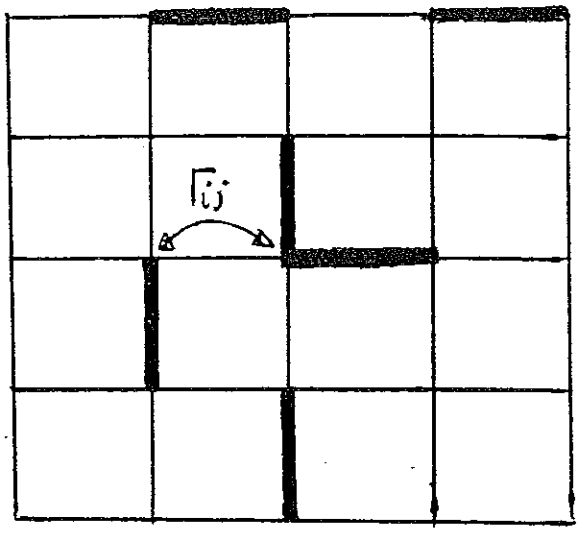

Figure 8: This shows the way the lattice is prepared with respect to active transition rates. The active transition rates are randomly selected and are identified by thick lines.

for large lattices ($\lim_{N\to\infty}$) at the bound percolation threshold. The percolation threshold P_c is the concentration P, at which an infinite cluster appears in an infinite lattice. In percolation theory, the RBM corresponds bond percolation. As described in Stauffer's book /25/, imagine each site of the lattice to be occupied, and lines drawn between neighboring lattice sites. Then each line can be an open bond with probability P, or a closed bond with $1-P$. A cluster is then a group of sites connected by open or activated bonds. A similar procedure with reverse process is described in /17,18/. That is, lattice with the removed bonds is like a board with a matrix of resistors some of which have been removed. After the random removal of each resistors a voltmeter measuring the resistance across the matrix is used to test

wether there is still a closed circuit. If the board is large enough (that is the number of resistors approaches infinity), the fraction of resistors at which the conductivity vanishes is a constant. This fraction is called the percolation concentration. Below this concentration there is no infinite cluster of connected resistors; whereas above this concentration there is certainly an infinite cluster. Even though not all bonds are contained in the infinite cluster, it does connect the opposite sides of the matrix as the number of sites goes to infinity. In our case we look for the critical concentration at which our lattice conducts for the first time. Call the hopping rate that completes the connection Γ^c_{ij}. The critical rate Γ^c_{ij} represents an estimate for the effective hopping rate of this disordered lattice, making an adaptation of argument of Ambegaokar, et al. /26/ .

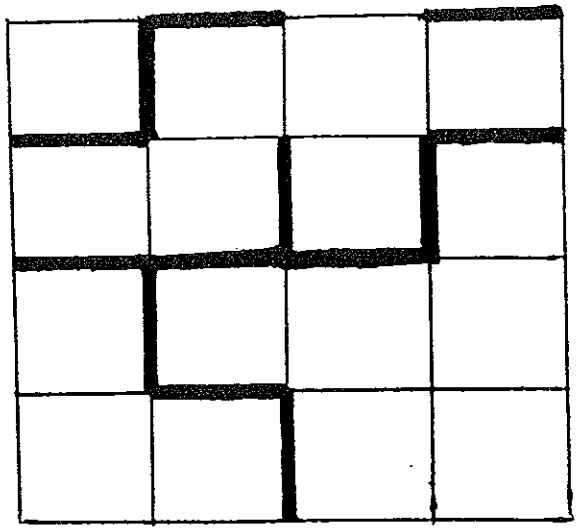

Figure 9: Here we see that the active bonds start to make a continous path for the first time which goes between opposite boundaries. This happens at a critical concentration called percolation threshold.

More formally :

Let $W(\Gamma)$ be the probability that a randomly chosen bond in the complete lattice (all bonds active) has a hopping rate that is larger than Γ . The general form is

plotted as in fig.(10) and described below. Then Γ_{ij}^c is found from

$$W(\Gamma_{ij}^c) = P_c \tag{72}$$

The relation with the distribution of $\rho(\Gamma)$ is

$$\begin{aligned} W(\Gamma) &= 1 - \int_{\Gamma_{min}}^{\Gamma} d\Gamma' \, \rho(\Gamma') \\ W(\Gamma) &= \int_{\Gamma}^{\Gamma_{max}} d\Gamma' \, \rho(\Gamma'). \end{aligned} \tag{73}$$

In the specific form of the random-barrier model that we investigate, the primary

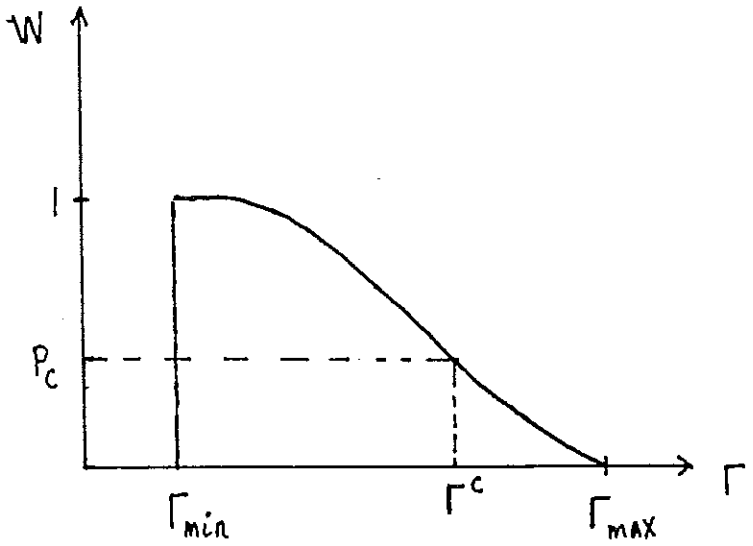

Figure 10: The distribution $w(\Gamma)$.

random variable is the energy of the barrier, not the hopping rate Γ_{ij} . Using the uniform distribution $\nu(E)$ of our model, the critical barrier height E_c is then derived. First, we use the condition

$$\rho(\Gamma)\, d\Gamma = -\nu(E)\, dE$$

equation (73) can be rewritten

$$
\begin{aligned}
W(E) &= 1 + \int_{E^*}^{E} dE' \nu(E') \qquad (74)\\
&= 1 - \int_{E}^{E^*} dE' \, \nu(E')\\
&= \int_{0}^{E^*} dE' \, \nu(E') - \int_{E}^{E^*} dE' \, \nu(E')\\
W(E) &= \int_{0}^{E} dE' \, \nu(E')
\end{aligned}
$$

substituting the value for $\nu(E')$ which is $\frac{1}{E^*}$, the integral yields

$$W(E) = \frac{E}{E^*} \qquad (75)$$

where $W(E)$ is probability that a randomly chosen bond has energy which is smaller than E. From the way $W(E)$ is defined $W(E_c)$ is given by

$$W(E_c) = P_c \qquad (76)$$

comparing equations (75) and (76) one finds the expression for the critical barrier

$$E_c = P_c \; E^* \qquad (77)$$

The prediction for the effective hopping is then

$$\Gamma(E_c) = \Gamma_{eff} = \Gamma_0 \exp\left(\frac{-P_c E^*}{K_B T}\right) \qquad (78)$$

If $E < P_c E^*$ barrier belongs to bonds that were used in the construction described above. The critical value for a continous path is at $P_c \, E^*$. For the bond percolation problem /25/

$$P_c = \begin{cases} 0.5 & d = 2 \;\; Square \; lattice \\ 0.242 & d = 3 \;\; Simple - Cubic \; lattice \end{cases} \qquad (79)$$

We compare the estimate for the effective hopping rate with the results of the EMT. In two dimensions both expressions agree, as equation (60) shows. In three

dimensions, equation (63) predicts an apparent activation energy of $0.333E^*$, while the percolation theoretical approach predicts an activation energy of $0.242E^*$. The comparison with simulations will be made on section 6.

5 Monte Carlo Simulations

5.1 General Description

We use a Monte Carlo algorithm to simulate the diffusion of the particle on disordered lattices. A disordered lattice is prepared by distributing lattice bond energies randomly according to the distribution equation (46). We calculate the corresponding transition rates using the Arrhenius law equation (47). Technically we proceed in $d = 1$ as follows. We put $\Gamma_0 = 0.5$, and calculate the transition probability PR to the right of, say, site i from the selected energy using equation (47). The left transition probability PL of site $i + 1$ is identical to the right transition rate PR of site i. At each site i, we divided the interval (0,1) into the sections (0,PR), (PR,PR+PL) and (PR+PL,1), using the values PR and PL assigned to this site. Once the probabilities are assigned to all sites, they remain "frozen"until the end of the program.

The particles are randomly distributed on the sites of the lattice and considered as independent. By taking many independent particles an ensemble average over many random walks is made. We work with one realization of the disordered lattice. For the random-barrier model we expect self-averaging properties, i.e., the random walk averages over many particles with different starting sites should also represent the disorder average.

During the dynamics, the particles are chosen randomly for possible transitions. This procedure ensures that the underlying stochastic dynamics of the individual transitions is Poissonian, and it is described in more detail in section 5.2. When a particle is selected, a random number is generated and compared with the subdivision of the interval (0,1) at the site where the particle is sitting. If the random number falls into the first section, the particle is moved to the right, if it falls to the second section, it is moved to the left, and if it falls into the third section, it

remains at this site. The extension to higher dimensions is obvious.

We have used periodic boundary conditions. If the particle happens to jump beyond the size of the lattice it is brought back to the original lattice for the purpose of determining the possible transition probabilities by subtracting or adding the length of the lattice. In that way we make the particle diffuse within a limited lattice size. In one dimension, we have used 25,600 particles on 12,800 sites. In two dimension the lattices are square lattices with dimension 400×400 and 25,600 of particles and in three dimension we considered cubic lattices with dimension $60 \times 60 \times 60$ and the number of particles is the same as in the other dimensions.

In every Monte Carlo step, the new position of each particle is stored or recorded. By following each step of the particle we are able to determine the mean–square displacement. When determining the mean–square displacement, we include displacements into the periodic continuations of the original lattice. That is, here we do not perform the reduction procedure described above. The usual time unit in Monte carlo simulations is the Monte Carlo step per particle (MCS/P); during one Monte Carlo step each particle is called once, on the average.

For the mobility simulations we use the same algorithm. The effects of the applied forces are reflected only in the transition rates. In one dimension when the system is made biased towards the positive X–direction, the corresponding transition rate is multiplied by the bias factor B and the transition rate in the negative X–direction is multiplied by B^{-1}. This favours particle diffusion along a prefered direction in our simulation. In one dimension the two possible directions are right and left. Hence the jump probability to the right PR is multiplied by B and the left jump probability PL is multiplied by B^{-1}. The procedure is easily extended to higher dimensions. As it is clear from the discussion above the mean displacement $\{R\}$ grows with the number of Monte Carlo steps. Therefore in the simulations we

monitor this parameter. All the other parameters such as number of particles and the lattice size remain unchanged. Of course, different values of α have been used.

5.2 Implementation of Poisson Process of Transitions on lattice with Disordered Rates (quenched disorder) by a Monte Carlo Procedure

In this subsection the random walk of a particle on a disordered lattice is considered where the transitions of the particle are assumed to represent a Poisson process in time. The transition rate from a site i to a nearest-neighbor site j will be called Γ_{ij}. The Sojourn probability of a particle at site i when particle can make transition to neighboring sites with rates Γ_{ij} in form of poisson process (time continous random walk which is described by master equation with constant rates) is given by

$$\Psi_i(t) = \exp\left[-\sum_{<j>_i} \Gamma_{ij} t\right]. \tag{80}$$

As the discrete random walk, so too the time-continous RW is a Markoffian process, that is, the present state is determined by the immediate past state at a particular time, but not by a more detailed sequence of states.

The MC procedure is required to reproduce this sojourn probability. We adopt the following procedure (adaptation of a procedure developed by K.Binder for Kawasaki dynamics); used for example by J.W.Haus, et al. /27,28/. An ensemble of N_p independent particles on the disordered lattice is introduced. Several particles can occupy the same site. This ensemble serves to implement the average over many particles. The particles are numbered and are called randomly. Within one Monte Carlo step, there are N_p calls. Consider one specific particle which resides on site i. Take the maximum transition rate from the set $\{\Gamma_{ij}\}$, called Γ_0, as the reference

rate. Define

$$P_{ij} = \frac{\Gamma_{ij}}{\Gamma_0}$$

$$P_i = \sum_{<j>_i} P_{ij} \quad and \quad r_i = 1 - P_i.$$

The probability that the specific particle is not selected in N_p call is

$$\left(1 - \frac{1}{N_p}\right)^{N_p} \tag{81}$$

The probability that the specific particle is selected m times in N_p calls, but it does not make any transition to a neighbor site is

$$\frac{N_p!}{m!(N_p - m)!}\left(1 - \frac{1}{N_p}\right)^{N_p - m}\left(\frac{r_i}{N_p}\right)^m .$$

The first factor is a combinatorial factor which represents the different possibilities to arrange the outcomes "not selected" and "selected, but no transitions". Since the events are mutually exclusive, the total probability of no transitions of the selected particle by N_p calls is

$$\begin{aligned} &\sum_{m=0}^{N_p}\binom{N_p}{m}\left(1 - \frac{1}{N_p}\right)^{N_p - m}\left(\frac{r_i}{N_p}\right)^m \\ &= \left(1 - \frac{1 - r_i}{N_p}\right)^{N_p} = \left(1 - \frac{P_i}{N_p}\right)^{N_p} \\ &\lim_{N_p \to \infty}\left(1 - \frac{P_i}{N_p}\right)^{N_p} = \exp(-p_i) \end{aligned} \tag{82}$$

Time is normally measured in MCS/P. The above result is for 1MCS/P, the generalization to t MCS/P is

$$\Psi_i(t) = \exp(-p_i\, t)$$

If time is measured in units of Γ_0^{-1}, we have

$$\Psi_i(t) = \exp\left(-\sum_{<j>_i} \Gamma_{ij}\, t\right)$$

Hence the required form of the sojourn probability is established, in the limit of large particle numbers N_p. It is clear from the description that a selected particle makes a transition to the neighboring site j with probability P_{ij} and a transition to any of the neighboring sites with probability P_i.

5.3 Waiting– Time Method

Here we describe another method, which has been introduced in /27/ and discussed, for example /28/. A particle makes a random walk on a bravais lattice; in this part only the stochastic process of the transition of the particle in time will be considered. The waiting time distribution (WTD) $\psi(t)$ of the particle is defined as follows. Let the particle have performed its last transition at $t = 0$. Then $\psi(t)$ is the probability density that it performs its next transition at time t after it waited until t. General WTD were introduced in the theory of random walks on lattices by Montroll and Weiss /29/. Transitions to neighboring sites according to a Poisson process where the sojourn probability is given by equation (80). $\sum_{<j>_i} \Gamma_{ij}$ is the summary rate for transitions from site i to neighboring sites j. For instance, at a specific site of a linear chain

$$\Psi(t) = \exp[-(\Gamma_r + \Gamma_l)t]$$

where the r and l stands for right and left respectively. In the waiting-time method, the time that a particle spends on a site is determined by randomly selecting a time out of a Poisson distribution which corresponds to the above sojourn probability. *General Procedure*: Let $f(x)$ be an exponential distribution,

$$f(x) = \frac{1}{\lambda}\exp(-\lambda\, x) \qquad\qquad x \geq 0$$

Let $\rho(y)$ be the uniform distribution

$$\rho(y) = \begin{cases} 1 & 0 \leq y \leq 1 \\ 0 & otherwise \end{cases} \tag{83}$$

The random numbers y are taken out of the uniform distribution, one obtains random numbers that are distributed according to the exponential distribution by

$$X = -\frac{1}{\lambda} ln(1-y).$$

Application to Hopping Process in Random Lattice (Random Barriers): The waiting time distribution for waiting at a site from 0 to t and then jump to the right or left neighbor is given by

$$\Psi_i(t) = (\Gamma_r + \Gamma_l) \exp(\Gamma_r + \Gamma_l)\, t \tag{84}$$

A random number y is generated and the corresponding waiting time is determined from

$$t = -\frac{1}{\Gamma_r + \Gamma_l} \ln(1-y) \tag{85}$$

time is measured in units of $2\Gamma_0$, that is $2\Gamma_0$ is considered as the unit time.

$$2\Gamma_0 t = -\frac{2\Gamma_0}{\Gamma_l + \Gamma_r} \ln(1-y) \tag{86}$$

$$2\Gamma_0 t = -\frac{1}{\frac{\Gamma_l}{2\Gamma_0} + \frac{\Gamma_r}{2\Gamma_0}} \ln(1-y)$$

($P_l = \frac{\Gamma_l}{2\Gamma_0}$, $P_r = \frac{\Gamma_l}{2\Gamma_0}$) are the probabilities for left or right jumps that are used in the first method of implementing the Poisson process. This method is much more difficult to implement than the first one, hence we did not use it for our simulations.

6 Results

Here we shall describe the results of our work. Results of simulations, analytical calculations and predictions of critical–path theory for the diffusion coefficient are disscussed below. Graphs for the mean–square displacement versus time in Monte Carlo steps are presented for different temperatures. However, the graphs for small temperature values (temperature refers to alpha) are disscussed separately. For these tempratures the asymptotic theoretical preditions are also shown. For the higher temperature curves we found it to be unneccessary to make this comparison, as the expected result is achieved in short Monte Carlo runs. Figure 11 describes the behaviour of the mean–square displacement $\{R^2\}$ as a function of time at different tempratures for one– dimensional lattices. We present data for the range of 10 to 10^5 MCS. We observe that for all temperatures there is always an early time regime which differs from the asymptotic regime where $R^2 \approx Dt$. That is at each temperature there exists a time that P.Argyrakis, et al. call cross over time τ_c /30/. In fig.11 we observe that for long times the log-log plot gives a linear relationship for $\alpha = 1, 0.5, 0.2$. As the temperature is reduced linearity is achieved at longer and longer times. For this reason high–temperature calculations are carried out to 10^3 steps. Figure 13 shows results of simulation and theory for 0.1, where corrections such as θ_1, θ_2 and θ_3 are included. The sense of concavity of the theoretical curve for small times is due to the divergence of the series (12) in the theoretcal expression for the mean–square displacement. But results for long time seem to agree reasonably.

Results of mobility simulation for one dimensional lattices are depicted in fig.12. Mean–square displacements versus time for two and three dimensional lattices are considered in fig.14 and fig.17 and a similar behaviour as in one dimension is observed. For a fixed temperature values it is observed that the diffusion coefficient for three dimensional lattices is the largest and for one dimensional lattices it is the

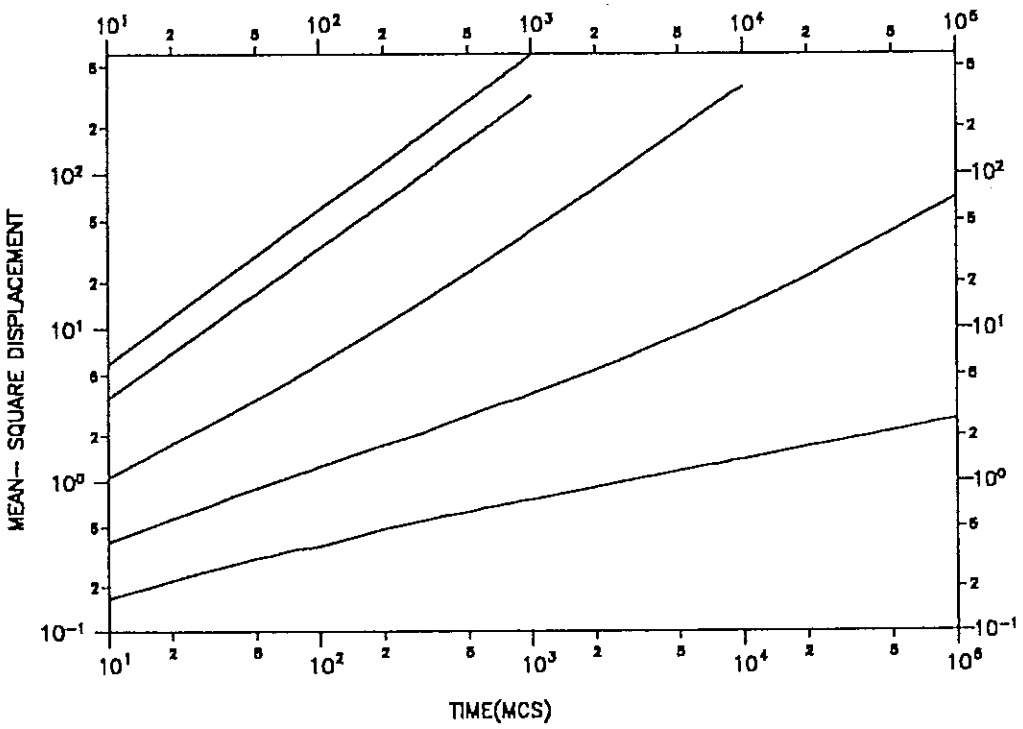

Figure 11: Mean-square displacement $\{R^2\}$ as a function of time (in MCs) for different temperatures (α values) for one dimensional lattices, in Log–Log form. Each curve corresponds to the following α values (top to bottom); 1.0, 0.5, 0.2, 0.1,0.05. These are results of diffusivty simulation for 25, 600 particles.

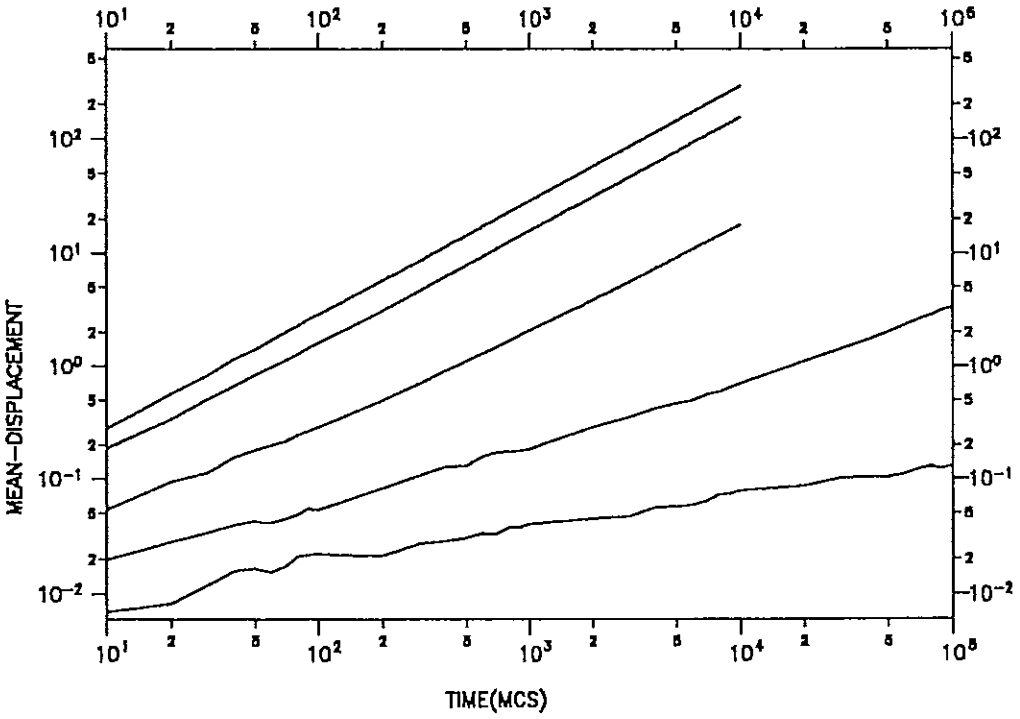

Figure 12: Mean–displacement $\{R\}$ as a function of time (in MCs) for different tempratures (α values) for one dimensional lattices, in Log–Log form. The curves correspond (top to bottom) to the following α values respectively; 1.0, 0.5, 0.2, 0.1, 0.05. These are results of mobility simulation for 25, 600 particles.

smallest, see table 1. In table 1 we tried to show values of diffusion coefficient calculated from three different methods; the EMT, diffusivity simulations, and mobility simulations for one, two, and three dimensional lattices. The variations are seen to be large (still less thau one percent) for small tempratures; 0.1 and 0.05. As it is said at the beginning graphs for small temperature values for two dimension and three dimension are considered in fig.16 and fig.19 respectively. A similar result is

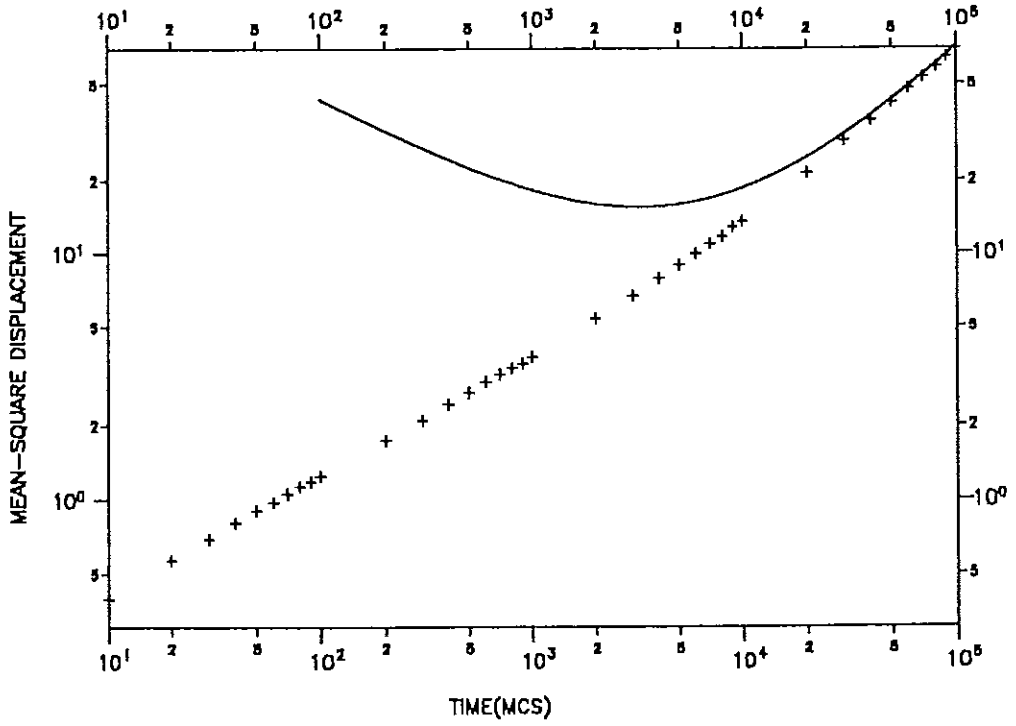

Figure 13: Plots of mean–square displacement from diffusivity simulation (crosses) for $\alpha = 0.1$ and theoretical curves in Log–Log form with the correction terms θ_1 ,θ_2 and θ_3 included for one dimensional lattice versus time (in MCs).

also observed from the mobility simulations and is considered in fig.15 and fig.18 for two and three dimension respectively. The asymptotic theoretical expression (42) for one dimension is plotted in smooth curve in fig. 13. The asymptotic curves for two and three dimensional lattices considered are results of the EMT (effective

medium theory). For two dimension, the diffusion coefficient for small α values is found to be $D^{EMT} = \Gamma_0 \exp \frac{-E^*}{2K_BT}$. Therefore, the mean-square displacement $\{R^2\}$ for long time limit would be

$$\{R^2\}(t) = 4D^{EMT}t$$

Similarly for three dimension the diffusion coefficient from EMT for small α is

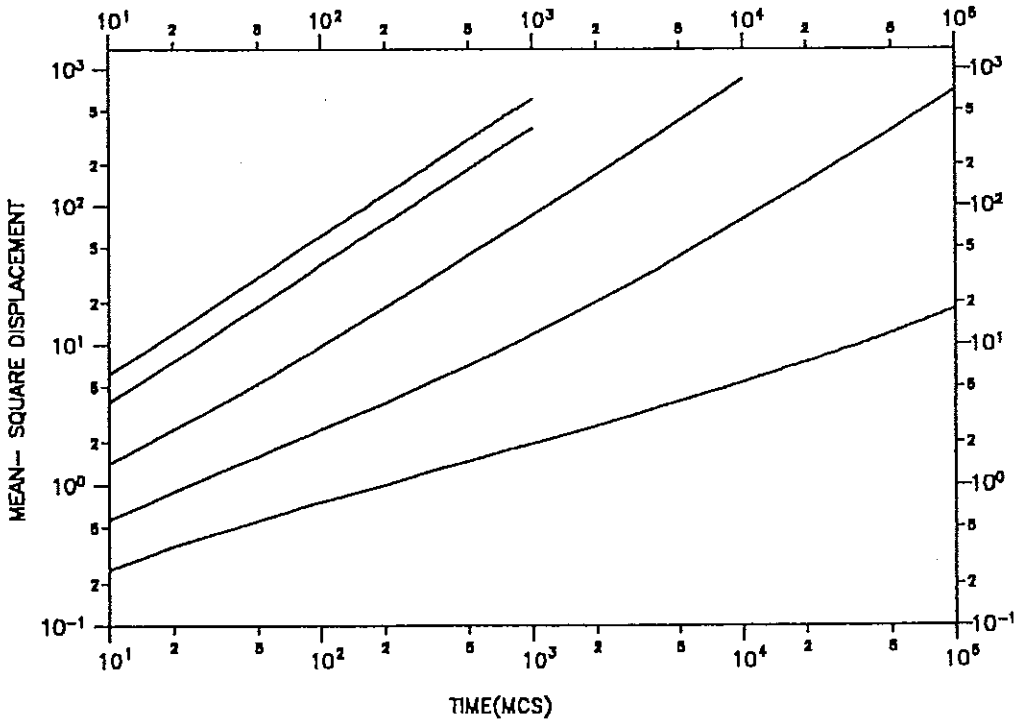

Figure 14: Mean-square displacement $\{R^2\}$ as a function of time (in MCs) for different temperatures (α values) for two dimensional lattices, in Log–Log form. Each curve corresponds to the following α values (top to bottom); 1.0, 0.5, 0.2, 0.1,0.05. These are results of diffusivty simulation for 25, 600 particles.

$D^{EMT} = \frac{\Gamma_0}{2} \exp \frac{-E^*}{3K_BT}$. And hence the–mean square displacement in the long time limit could be expressed as

$$\{R^2\} = 6D^{EMT}t$$

These two equations represents the asymptotic results that are plotted in fig.16 and 19, respectively. The temperature dependent cross-over time τ_c is described below.

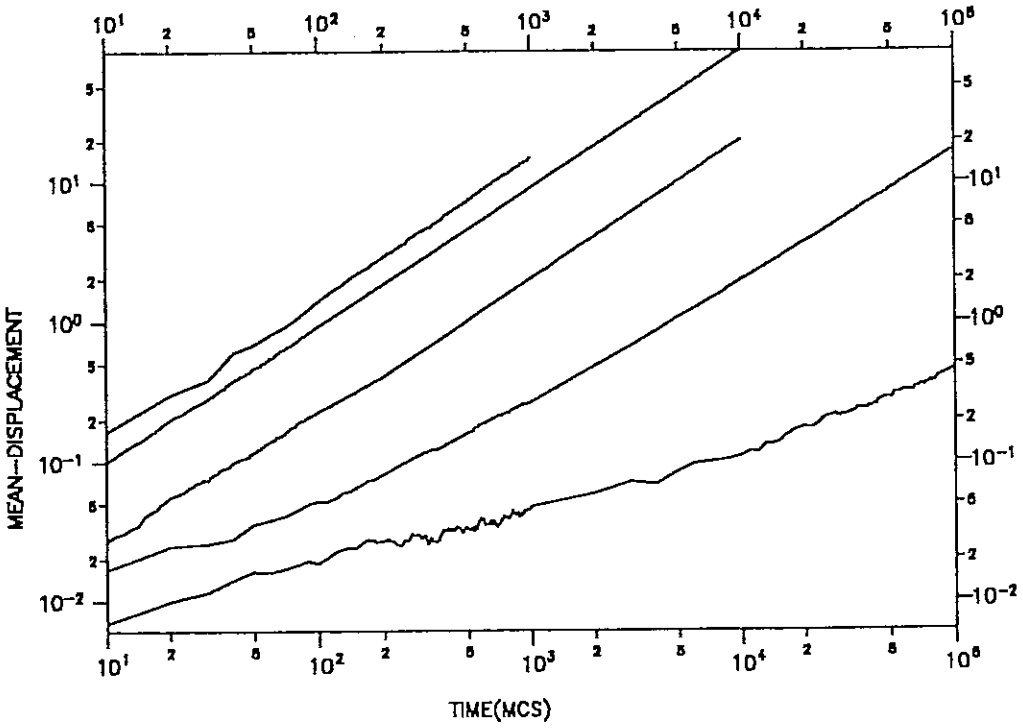

Figure 15: Mean-displacement $\{R\}$ as a function of time (in MCs) for different tempratures (α values) for two dimensional lattices, in Log-Log form. The curves correspond (top to bottom) to the following α values respectively; 1.0, 0.5, 0.2, 0.1, 0.05. These are results of mobility simulation for 25, 600 particles.

As the particle starts at some random position, it is most probable that it is localized at some relatively low energy valley at which it is to be found. Thus at early times and low temperatures the particle is 'trapped' in some limited region of the lattice and can not escape at low temperature and all jumps are consumed to visit the same sites over and over again. The probability of escaping is very small, but after

a given time τ_c this probability is realized. It is expected that the cross over time is

$$\tau_c = \exp \frac{E_c}{K_B T}. \tag{87}$$

Argyrakis, et al. estimated the cross over time τ_c for each temperature /30/.

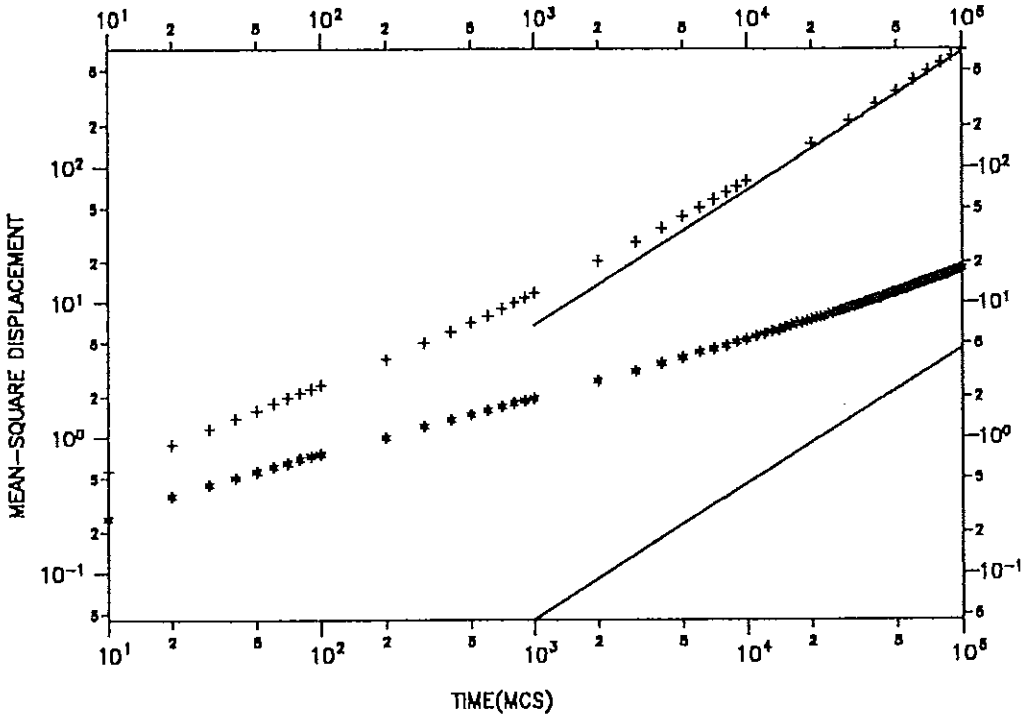

Figure 16: Mean-square displacement from diffusivity simulation for $\alpha = 0.1$,0.05 and theoretical asymptotic results of EMA for the same α values in two dimension. Simulation results are crosses and astrik for 0.1 and 0.05 respectively.

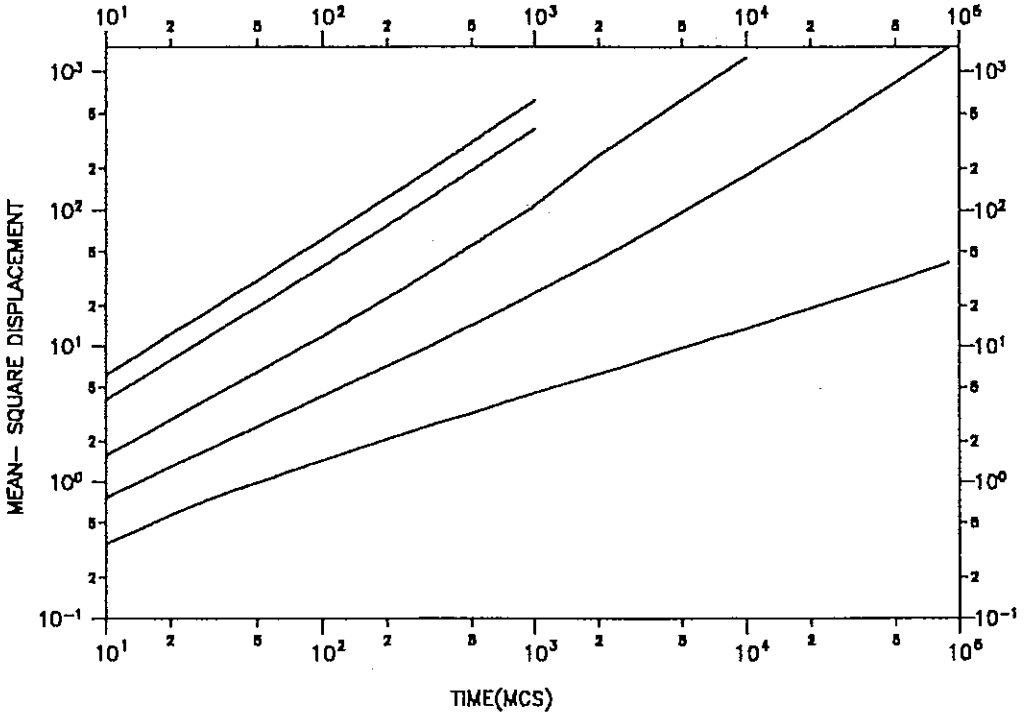

Figure 17: Mean-square displacement $\{R^2\}$ as a function of time (in MCs) for different temperatures (α values) for three dimensional lattices, in Log-Log form. Each curve corresponds to the following α values (top to bottom); 1.0, 0.5, 0.2, 0.1,0.05. These are results of diffusivty simulation for 25, 600 particles.

Comparison of Values of Diffusion Coefficient from Different Methods

α	EMT			Diffusivity Simulation			Mobility Simulation		
	d = 1	d = 2	d = 3	d = 1	d = 2	d = 3	d = 1	d = 2	d = 3
1	$0 \cdot 291$	$0 \cdot 152$	$0 \cdot 102$	$0 \cdot 295$	$0 \cdot 151$	$0 \cdot 103$	$0 \cdot 284$	$0 \cdot 148$	$0 \cdot 1$
0.5	$0 \cdot 157$	$9 \cdot 197 \times 10^{-2}$	$6 \cdot 475 \times 10^{-2}$	$0 \cdot 160$	$9 \cdot 229 \times 10^{-2}$	$6 \cdot 42 \times 10^{-2}$	$0 \cdot 153$	$8 \cdot 943 \times 10^{-2}$	$6 \cdot 287 \times 10^{-2}$
0.2	$1 \cdot 696 \times 10^{-2}$	$2 \cdot 052 \times 10^{-2}$	$1 \cdot 871 \times 10^{-2}$	$1 \cdot 826 \times 10^{-2}$	$2 \cdot 09 \times 10^{-2}$	$2 \cdot 093 \times 10^{-2}$	$1 \cdot 76 \times 10^{-2}$	$1 \cdot 989 \times 10^{-2}$	$1 \cdot 66 \times 10^{-2}$
0.1	$2 \cdot 270 \times 10^{-4}$	$1 \cdot 684 \times 10^{-3}$	$3 \cdot 079 \times 10^{-3}$	$3 \cdot 5 \times 10^{-4}$	$1 \cdot 751 \times 10^{-3}$	$2 \cdot 733 \times 10^{-2}$	$3 \cdot 381 \times 10^{-4}$	$1 \cdot 69 \times 10^{-3}$	$1 \cdot 434 \times 10^{-3}$
0.05	$2 \cdot 06 \times 10^{-8}$	$1 \cdot 13 \times 10^{-5}$	$1 \cdot 062 \times 10^{-4}$	$1 \cdot 278 \times 10^{-5}$	$4 \cdot 474 \times 10^{-5}$	$7 \cdot 63 \times 10^{-5}$	$1 \cdot 304 \times 10^{-5}$	$1 \cdot 42 \times 10^{-5}$	$2 \cdot 209 \times 10^{-5}$

Table 1

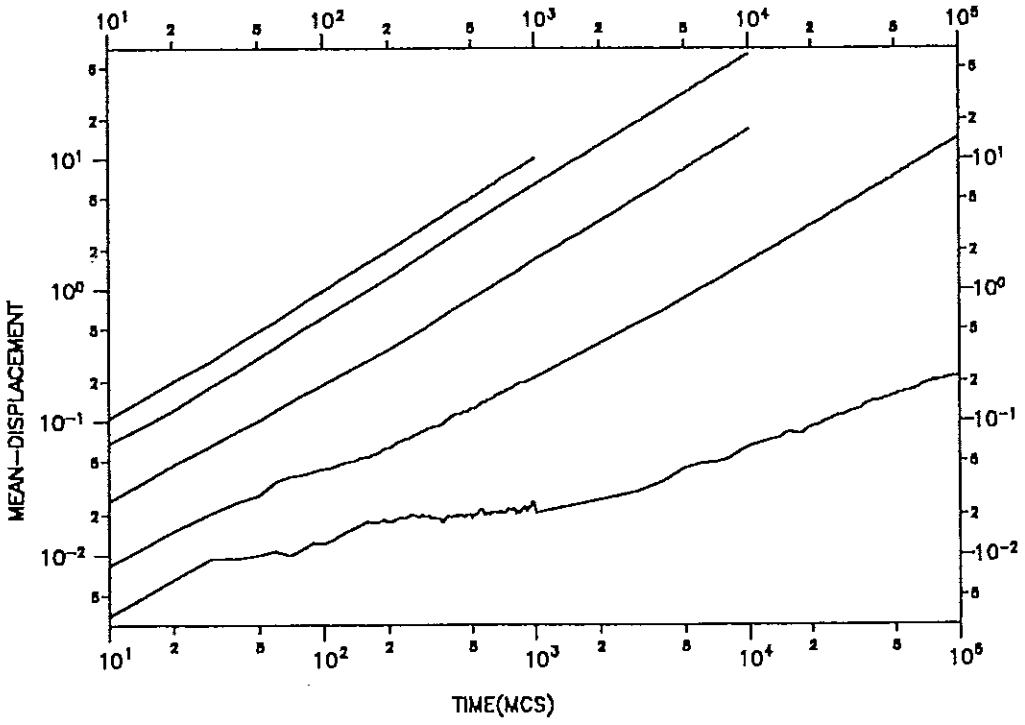

Figure 18: Mean-displacement $\{R\}$ as a function of time (in MCs) for different tempratnres (α values) for three dimensional lattices, in Log–Log form. The curves correspond (top to bottom) to the following α values respectively; 1.0, 0.5, 0.2, 0.1, 0.05. These are results of mobility simulation for 25, 600 particles.

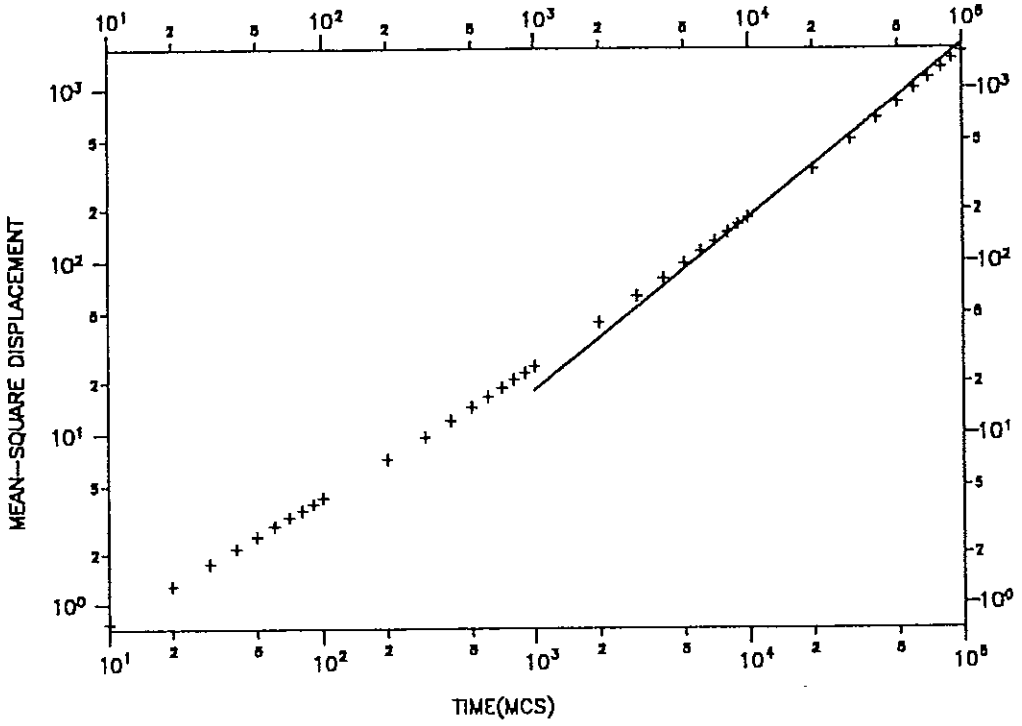

Figure 19: Mean-square displacement from diffusivity simulation (crosses) for $\alpha = 0.1$ and asymptotic results from EMA for the same α value for three dimensional lattices.

7 Discussion and Conclusion

This work demonstrates the influence of degree of disorder (α) on the diffusivity behaviour of particles in media with static disorder which is realized by energy barrier distributions. It has been observed to have much influence at low temperatures. It is observed that the Monte Carlo simulations give the largest diffusion coefficient for three dimensions followed by two dimensions, and the smallest diffusion coefficient for one dimension, if instead of the normalization $\Gamma_0 = \frac{1}{z}$ the more physical normaliztion $\Gamma_0 = 1$ is used. The EMT also gives the same result. The reason is the larger the lattice dimension, the higher is the chance for the particle to find smaller barriers to percolate through the lattice.

For systems with a bias (non– equilibrium situation), the diffusion coefficient obtained is reasonably close to the predictions and results of the other methods. However, graphs of mobility simulation seem to be noisy. It is a problem of improving the statistics. One should be able either to increase the number of particles or to increase the number of Monte Carlo steps. The same problem has been observed in the case of diffusivity simulation. For the smaller α values the asymptotic behavior is not yet completely reached in 10^5 MCS. Larger number of Monte Carlo steps would require too much computing time. It is this constraint that limited us to a maximum of 10^5 MCS. In fig.16 for $\alpha = 0.05$ it seems that the diffusivity regiem is not yet reached but the tendency has already been started to be observed around 10^5. The asymptotic regiem would be achieved if one goes to higher MCs. Simulations will have always statistical errors, and the problem seen in fig.19 ; the overlapping of simualtion with the asymptotic EMT curve for $\alpha = 0.1$ for three dimensional lattices I think is its effect. The deviations observed in table 1 for $\alpha = 0.1$ and 0.05 between EMT and Simulation results are mainly statistical and due to short or limited MCs considered. The analytical results from EMT are in a good agreement with the

Monte Carlo simulations. The predictions of EMT and critical path argument agree in one, two dimensions and disagree in three dimension. Our simulations agree with EMT in three dimensions, not with the result of the critical–path arguments. However one must note that we have the critical-path argument in its simplest form. It has been improved in recent work /23,24/. On the other hand it has been shown by Luck /17/ by using perturbation theory that the EMT is accurate up to the fourth order. In any case, the parameter values α where the asymptotic regime is reached, the EMT clearly provides an adequate description.

Appendices

Appendix A

Here you find the derivation of $\tilde{E}_0$. From equation (9) of section 2 it is given by

$$\tilde{E}_0(s) = \frac{1}{\pi}\int_{-\pi}^{\pi} \frac{dk}{s + 2\,\tilde{\Gamma}(s)(1 - cosk)} \tag{88}$$

making some rearangements and denotting

$$b = \frac{s}{2\,\tilde{\Gamma}(s)} + 1$$

$\tilde{E}_0(s)$ can be expressed as

$$\frac{1}{2\pi\,\tilde{\Gamma}(s)}\int_{-\pi}^{\pi} \frac{dk}{b - cosk} \tag{89}$$

the integral can be converted into contour integral in complex plane by setting $Z = \exp(ik)$. Then

$$\begin{aligned} dk &= \frac{dZ}{iZ} \\ cosk &= \frac{1}{2}\left(Z + \frac{1}{Z}\right) \end{aligned}$$

and substituting these

$$\tilde{E}_0(s) = \frac{1}{\pi\,\tilde{\Gamma}(s)}\int_c \frac{dZ}{i\,[Z - (b + (b^2-1))^{\frac{1}{2}}][Z - (b - (b^2-1))^{\frac{1}{2}}]} \tag{90}$$

The integrand has two poles: at $Z = b + (b^2-1)^{\frac{1}{2}}$ and $Z = b - (b^2-1)^{\frac{1}{2}}$. If $b > 1$, the second pole is inside the contour. So, only the residue at this value is needed; it is equal to

$$\frac{1}{i}\,\frac{1}{2(b^2-1)^{\frac{1}{2}}}$$

therefore

$$\tilde{E}_0(s) = 2\pi i\left[\frac{1}{2\pi i\,\tilde{\Gamma}(s)}\,\frac{1}{(b^2-1)^{\frac{1}{2}}}\right] \tag{91}$$

Finally it is arrived at the desired result

$$\tilde{E}_0 = \frac{1}{[s^2 + 4s\,\tilde{\Gamma}(s)]^{\frac{1}{2}}} \tag{92}$$

and hence

$$\lim_{s\to 0} s\,\tilde{E}_0(s) \to 0$$

Appendix B

$\tilde{E}_{00}(s)$ is expressed using equation (27) as follows

$$\tilde{E}_{00} = \frac{1}{\pi^2}\int_0^\pi \int_0^\pi dx\,dy \frac{1}{s + 4\tilde{\Gamma}(s) - 2\tilde{\Gamma}(s)cosx - 2D(s)cosy} \tag{93}$$

Here, x and y stands for k_1 and k_2 respectively. Making some rearangements and denotting a to be

$$a = 2 + \frac{s}{2\tilde{\Gamma}(s)} - cosx$$

it is reduced to

$$\tilde{E}_{00} = \frac{1}{2\tilde{\Gamma}(s)\pi}\int_0^\pi dx \frac{1}{\pi}\int_0^\pi dy \frac{1}{a - cosy}\,.$$

the result of the inner integral with respect to y is already shown in appendix A. Then implementing that, results in

$$\tilde{E}_{00} = \frac{1}{2\tilde{\Gamma}(s)\pi}\int_0^\pi dx \frac{1}{\sqrt{(2 + \frac{s}{2D} - cosx)^2 - 1}} \tag{94}$$

$$\tilde{E}_{00} = \frac{1}{2\tilde{\Gamma}(s)\pi}\int_0^\pi dx \frac{1}{\sqrt{(2 + \frac{s}{2\tilde{\Gamma}(s)})^2 - 1 - 2(2 + \frac{s}{2\tilde{\Gamma}(s)})\,cosx + cos^2x}}$$

Let,

$$t = tan\frac{x}{2} \tag{95}$$

then

$$cosx = \frac{1 - t^2}{1 + t^2}$$

$$dx = \frac{2}{1 + t^2}\,dt$$

$$\tilde{E}_{00}= \frac{1}{2\,\tilde{\Gamma}\,(s)\pi}\int_0^\infty dt\,\frac{1}{\sqrt{[(2+\frac{s}{2\tilde{\Gamma}(s)})^2-1]\,(1+t^2)^2-2(2+\frac{s}{2\tilde{\Gamma}(s)})(1-t^2)\,(1+t^2)+(1-t^2)}} \tag{96}$$

It is now a polynomial of fourth order in the square root, so it can be reduced to an elliptical integral. Finding first zeros of the polynomial:

$$at^4+bt^2+c=0 \tag{97}$$

the roots are,

$$t_+^2 = -\frac{\frac{s}{2\tilde{\Gamma}(s)}}{2+\frac{s}{2\tilde{\Gamma}(s)}}$$

$$t_-^2 = -\frac{2+\frac{s}{2\tilde{\Gamma}(s)}}{4+\frac{s}{2D}}$$

where,

$$a = (2+\frac{s}{2\,\tilde{\Gamma}\,(s)})(4+\frac{s}{2\,\tilde{\Gamma}\,(s)})$$

$$b = \left[(2+\frac{s}{2\,\tilde{\Gamma}\,(s)})^2-2\right]$$

$$c = \frac{s}{2\,\tilde{\Gamma}\,(s)}(2+\frac{s}{2\,\tilde{\Gamma}\,(s)})$$

$$\tilde{E}_{00}= \frac{1}{\tilde{\Gamma}\,(s)\pi}\int_0^\infty dt\,\frac{1}{\sqrt{(2+\frac{s}{2\tilde{\Gamma}(s)})(4+\frac{s}{2\tilde{\Gamma}(s)})(t^2+\frac{\frac{s}{2D}}{2+\frac{s}{2D}})(t^2+\frac{2+\frac{s}{2\tilde{\Gamma}(s)}}{4+\frac{s}{2\tilde{\Gamma}(s)}})}}\,. \tag{98}$$

Now define:

$$\alpha^2 = -t_-^2$$

$$\beta^2 = -t_+^2$$

$$\tilde{E}_{00}= \frac{1}{\tilde{\Gamma}\,(s)\pi\sqrt{a}}\int_0^\infty dt\,\frac{1}{\sqrt{(t^2+\alpha^2)\,(t^2+\beta^2)}} = \frac{1}{\tilde{\Gamma}\,(s)\pi\sqrt{a}}\,\frac{1}{\alpha}\,F(\frac{\pi}{2},\frac{\sqrt{\alpha^2-\beta^2}}{\alpha}) \tag{99}$$

for the integrals see Ryshik–Gradstein /31/. From the properties of elliptic integral, we have

$$F(\frac{\pi}{2},k)=K(k)$$

where,

$$k = \frac{\sqrt{\alpha^2 - \beta^2}}{\alpha} = \frac{2}{2 + \frac{s}{2\tilde{\Gamma}(s)}}$$

$$\frac{1}{\alpha} = \frac{\sqrt{a}}{2 + \frac{s}{2\tilde{\Gamma}(s)}}$$

$$\tilde{E}_{00} = \frac{2K(k)}{2\,\tilde{\Gamma}\,(s)\pi(2 + \frac{s}{2\tilde{\Gamma}(s)})} \tag{100}$$

$$K(k) = K(k')$$

$$k' = \sqrt{1 - k^2}$$

see /31/ for the general properties of elleptical integral. Representation by series (Ryshik Gradstein 6.113)

$$K(k') = \ln \frac{4}{k'} + \frac{1}{4}\left(\ln \frac{4}{k'} - 1\right) k'^2 + \cdots \tag{101}$$

for small s, $\lim_{s\to 0} k' = \sqrt{\frac{s}{2\tilde{\Gamma}(s)}}$. Then,

$$\lim_{s\to 0} \tilde{E}_{00}\,(s) = \frac{1}{4\pi\,\Gamma_{eff}} \ln \frac{16}{\frac{s}{2\tilde{\Gamma}_{eff}}} \tag{102}$$

Appendix C

Here we show the corrections to linear diffusivity in one and two dimension. The correction parameters for one dimension diffusion coefficients such as θ_1, θ_2 and θ_3 which are results of EMA as given by J.W.Haus and K.W.Kehr /14/ are shown in table below

θ_1	θ_2	θ_3
$\frac{k_2}{2}$	$\frac{-k_3}{4} + 3\frac{k_2^2}{8}$	$\frac{k_4}{8} - \frac{k_2}{16} - 7\frac{k_2 k_3}{16} + \frac{21 k^3{}_2}{64}$

Table 2.

where,

$$k_2 = \frac{\left\{\left(\frac{1}{\Gamma} - \left\{\frac{1}{\Gamma}\right\}\right)^2\right\}}{\left\{\frac{1}{\Gamma}\right\}^2}$$

$$k_3 = \frac{\left\{\left(\frac{1}{\Gamma} - \left\{\frac{1}{\Gamma}\right\}\right)^3\right\}}{\left\{\frac{1}{\Gamma}\right\}^3}$$

$$k_4 = \frac{\left\{\left(\frac{1}{\Gamma} - \left\{\frac{1}{\Gamma}\right\}\right)^4\right\}}{\left\{\frac{1}{\Gamma}\right\}^4}$$

The linear correction to the diffusion coefficient in two dimension is derived as follows /14/: The diffusion coefficient is now can be written

$$\Gamma(s) = \Gamma_{eff}(1 + \varphi(s)) \tag{103}$$

$\varphi(s)$ is the correction term. It is small when s goes to zero. substituting this into the self consistency condition for two dimension equation (30) in section 2,

$$\left\{\frac{\Gamma_{eff}(1+\varphi(s)) - \Gamma'}{\Gamma_{eff}(1+\varphi(s)) + \Gamma' + s\ \tilde{E}_{00}(s)[\Gamma_{eff}(1+\varphi(s)) - \Gamma']}\right\}_{\rho(\Gamma')} = 0 \tag{104}$$

$\varphi(s)$ and $s\ \tilde{E}_{00}(s)$ small for s goes to zero. And expansion with respect to these quantities enables $\varphi(s)$ to be

$$\varphi(s) = s\ \tilde{E}_{00}(s) q \tag{105}$$

where q is

$$q = \frac{\left\{\frac{\left(1-\frac{\Gamma'}{\Gamma_{eff}}\right)^2}{\left(1+\frac{\Gamma'}{\Gamma_{eff}}\right)^2}\right\}}{\left\{2\frac{\frac{\Gamma'}{\Gamma_{eff}}}{(1+\frac{\Gamma'}{\Gamma_{eff}})^2}\right\}} \tag{106}$$

The diffusion coefficient becomes then,

$$\Gamma(s) = \Gamma_{eff}\left[1 + \theta_2 \ln\frac{16}{\frac{s}{2\Gamma_{eff}}}\right] \tag{107}$$

θ_2 being expressed as

$$\theta_2 = q\frac{s}{4\pi\Gamma_{eff}} \tag{108}$$

Here we used results of appendix B for $\widetilde{E}_{00}(s)$.

References

/1/ H.A. Kramers, Physica 7 (1940) 284.

/2/ G.H. Vineyard,J. Phys. Chem. Sol. 3 (1957) 121.

/3/ H. Haken, Laser Theory (Spriger, Berlin, 1984).

/4/ L. Arnold and R. Lefever, eds., Stochastic non Linear Systemsin Physics, Biology, Springer series in Synergetics 8 (Spriger, Berlin, 1981).

/5/ G. Grinstein and J.F. Fernandez,Phys. Rev. B29 (1984) 6389.

/6/ S. Havlin and D.Ben-Avraham, Adv. Phys., 36(1987) 697.

/7/ K. Binder and A.P. Young, Rev. Mod. Phys. 58 (1986) 801.

/8/ R. Kopelman, J. Statist. Phys. A, 42 (1986) 185.

/9/ J. Bernasconi, H.U. Beyeler, S. Strässler, and S. Alexander, Phys. Rev. Lett. 42 (1979) 816.

/10/ J.P. Bouchaud, and A. Georges, Phys. Rep. 195 (1990) 127.

/11/ R.J. Elliot, J.A. Krumhansl and P.L. Leath, Rev. Mod. Phys. 46 (1974) 465.

/12/ S. Alexander and R. Orbach, J. Phys. Lett., 43 (1982) 625.

/13/ J.W. Haus and K.W. Kehr, Phys. Rep. 150 (1987) 263.

/14/ G.H. Weiss and R.J. Rubin, Adv. Chem. Phys., 52 (1983)363.

/15/ I. Webman, Phys. Rev. Lett., 47 (1981) 1496.

/16/ J.W. Haus, K.W. Kehr, and K. Kitahara, Phys. Rev. B25 (1982) 4918.

/17/ J.W. Luck, Phys. Rev. B43 (1991) 4341.

/18/ S. Kirpatrik, Rev. Mod. Phys., 45 (1973) 574.

/19/ J.W. Haus and K.W. Kehr,Phys. Rev. B44 (1991)4341.

/20/ T. Odagaki and M. Lax, Phys.Rev. B24 (1981) 5284.

/21/ C.K. Hu and H.B. Huntington, Phys. Rev. B26 (1982) 2782.

/22/ H.G. Haubold, Rev. Phys. Appl. 11 (1976) 73.

/23/ S. Tyc and B.I. Halperin, Phys. rev. B39 (1989) 877.

/24/ P. Le Doussal, Phys. Rev. B39 (1989) 881.

/25/ D. Stauffer, Introduction to Percolation Theory, 1985.

/26/ V. Ambegaokar, B.I. Halperin and J.S. Langer, Phys. Rev. B4 (1971) 2612.

/27/ K. Binder, Phys. Rev. B15 (1977) 4425.

/28/ J.W. Haus and K.W. Kehr, Phys. Rev. B28 (1983) 6.

/29/ E.W. Montroll and G.H. Weiss, J. Math. Phys. 6 (1965) 167.

/30/ I. Avramov, A. Milchev and P. Argyrakis, Phys. Rev. E47 (1993)2303.

/31/ I.M. Ryshik, I.S. Gradstein, Tables of series, products, and integrals (1957).